

## General Disclaimer

### One or more of the Following Statements may affect this Document

- This document has been reproduced from the best copy furnished by the organizational source. It is being released in the interest of making available as much information as possible.
- This document may contain data, which exceeds the sheet parameters. It was furnished in this condition by the organizational source and is the best copy available.
- This document may contain tone-on-tone or color graphs, charts and/or pictures, which have been reproduced in black and white.
- This document is paginated as submitted by the original source.
- Portions of this document are not fully legible due to the historical nature of some of the material. However, it is the best reproduction available from the original submission.

## LEGAL NOTICE

This report was prepared as an account of Government sponsored work. Neither the United States, nor the Commission, nor any person acting on behalf of the Commission:

A. Makes any warranty or representation, expressed or implied, with respect to the accuracy, completeness, or usefulness of the information contained in this report, or that the use of any information, apparatus, method, or process disclosed in this report may not infringe privately owned rights; or

B. Assumes any liabilities with respect to the use of, or for damages resulting from the use of any information, apparatus, method, or process disclosed in this report.

As used in the above, "person acting on behalf of the Commission" includes any employee or contractor of the Commission, or employee of such contractor, to the extent that such employee or contractor of the Commission, or employee of such contractor prepares, disseminates, or provides access to, any information pursuant to his employment or contract with the Commission, or his employment with such contractor.

ORNL-TM-1550

CYSTE PRICES

BIOLOGY DIVISION

### SYNERGISTIC EFFECT OF ZERO-G AND RADIATION ON WHITE BLOOD CELLS

H.C. \$ 2.00; MN .50

An Experiment for the  
Gemini III Manned Space Flight

Annual Report  
Period Ending June 30, 1965

Prepared by  
M. A. Bender

RELEASED FOR ANNOUNCEMENT  
IN NUCLEAR SCIENCE ABSTRACTS

This research is carried out at ORNL under NASA Order Number R-104 Task 4

AUGUST 1966

OAK RIDGE NATIONAL LABORATORY  
Oak Ridge, Tennessee  
operated by  
UNION CARBIDE CORPORATION  
for the  
U. S. ATOMIC ENERGY COMMISSION

## SUMMARY

This report describes work performed through June 30, 1965, on an experiment entitled "Synergistic Effect of Zero-G and Radiation on White Blood Cells," also known as "Experiment S-4." The experiment was carried out at the request of the National Aeronautics and Space Administration under an interagency agreement between that agency and the U.S. Atomic Energy Commission. The work included the design and execution of the experiment, which was successfully carried out during the Gemini III manned space flight of March 23, 1965, and the fabrication of the experimental hardware. The S-4 experiment consisted of the irradiation of samples of human leukocytes with  $^{32}\text{P}$  beta particles during the orbital phase of the mission, and the subsequent cytogenetic analysis of the material to determine chromosomal aberration rates. Preparation of the experiment included the design, fabrication, and testing of the necessary hardware and equipment.

The project was begun during January 1964. Progress through June 30, 1964, has been described in ORNL-TM-940. The first 8 months of FY 1965 were devoted to fabrication and testing of the flight hardware and preparation of the required documentation. During this period additional biological, radiological, and physical testing, including a series of mock-up executions of the experiment, were completed. Deployment of equipment and personnel in the launch and recovery areas began several weeks before the flight. Analysis of the experimental material and of the instrumentation, and statistical analysis of the data were completed during the 3 months following the flight.

The experimental data showed that although there was no significant difference between the yields of multiple-break aberrations induced on the ground and induced during orbital flight, the frequency of single-break aberrations was significantly higher in the flight samples. Several lines of evidence rule out the possibility that this difference arose from differences in absorbed dose, temperature, oxygen tension, or other parameters known to influence chromosome aberration yields. That the space flight itself induced aberrations is ruled out by the experiment control samples and also by preflight and postflight blood samples obtained from the Gemini III flight crew. A synergism between radiation and some space-flight parameter thus appears to exist for human chromosome aberration production.

## CONTENTS

SUMMARY .....	iii
I. INTRODUCTION .....	1
II. ORGANIZATION .....	2
III. PREPARATION OF THE EXPERIMENT .....	3
A. The Experimental Device .....	3
B. Instrumentation .....	6
C. Supporting Equipment.....	8
D. Dosimetry .....	9
E. Mock-up Experiments .....	22
IV. EXECUTION OF THE EXPERIMENT .....	27
A. Preflight.....	27
B. Flight .....	28
C. Postflight.....	28
V. EXPERIMENTAL RESULTS .....	30
A. Instrumentation Packages .....	30
B. Dosimetry .....	31
C. Biological .....	35
D. Discussion.....	37



## I. INTRODUCTION

Work on the S-4 experiment was started on January 15, 1964, and the work done up to June 30, 1964, has been described in the annual report of the project for fiscal year 1965 (ORNL-TM-940). During that period the definitive experimental plan, the design of the experimental hardware, and most of the testing and qualification documentation were completed. The Oak Ridge Y-12 Plant had begun fabrication of the actual flight hardware, and much of the equipment necessary for the preflight preparation and the postflight handling of the experiment had been procured or fabricated.

The period covered by the present report included the actual execution of the S-4 experiment in conjunction with the GT-3 mission of March 23, 1965. The work accomplished can most conveniently be described separately for the periods before, during, and following the actual experiment.

In the period prior to launch all hardware and equipment fabrication, testing, and documentation were completed. A series of mock-up experiments were also carried out, as far as possible under the same conditions, and using the same hardware, equipment, and facilities as anticipated for the actual experiment. These mock-ups provided training and practice for the personnel involved, as well as backup ground control data. Beginning several weeks prior to the mission, personnel, equipment, and special facilities were deployed to the launch and recovery areas. A specially equipped trailer for laboratory and assembly work was located at Cape Kennedy. One biologist with portable equipment was located on the prime recovery vessel and on each of two contingency area vessels.

Following the flight the cytological preparations and the experimental devices were returned to Oak Ridge. The dosimeters were read, and the recovered devices with their original  $^{32}\text{P}$  sources were used for further dosimetric determinations. The instrumentation packages and their temperature and activation records were analyzed. A total of 4600 cells from the experimental and flight crew samples were analyzed for chromosomal aberrations. The resulting data were analyzed statistically, and evidence for a synergism between the  $\beta$  radiation and some unidentified space-flight parameter was obtained.

## II. ORGANIZATION

Preparation and execution of the S-4 experiment required the close cooperation of several different Oak Ridge organizations. Design, fabrication, and testing of the experimental device and of the necessary supporting equipment, and the engineering aspects of the execution of the experiment were the responsibility of the Oak Ridge Y-12 Plant. The isotopic  $\beta$ -radiation sources were fabricated by the Isotopes Division of the Oak Ridge National Laboratory. The conceptual design of the experiment and the biological and dosimetric portions of the experiment were the responsibility of the Biology Division of the Oak Ridge National Laboratory. The individuals directly responsible for the various phases of the work were as follows:

Principal Investigator: M. A. Bender, Biology Division, ORNL

Physical Design, Fabrication, and Testing: H. F. Smith, Jr.,  
Oak Ridge Y-12 Plant

Mechanical: W. T. Smith, Jr.

Testing: W. W. Lee

Instrumentation: S. E. Groothuis

Isotope Sources: F. N. Case, Isotopes Division, ORNL

Biology: P. C. Gooch, Biology Division, ORNL

Radiological Physics: S. Kondo, Department of Fundamental  
Radiology, Faculty of Medicine, Osaka University,  
Osaka, Japan (on assignment to ORNL)

### III. PREPARATION OF THE EXPERIMENT

#### A. The Experimental Device

The design and qualification of the experimental device had already been completed by June 30, 1964. The only modification made after that time was in the method of application of the radioisotope to the source-plate assemblies as described below. Sufficient quantities of parts for the experimental device were fabricated to provide for practice experiments and tests as well as for flight and backup devices. Use of tape-controlled equipment (Fig. 1) greatly facilitated the machining of the final parts. The flight and backup hardware was inspected and certified as GFA equipment. In addition, a number of housings were made without the internal milling. These were used for test and practice of the field welding operation required during final assembly of the experimental devices just before flight.

**$^{32}\text{P}$  Source-Plate Assemblies.** — The original method of producing the  $^{32}\text{P}$  layer on the platinum foil source-plate discs was to deposit an aliquot of a solution of potassium silicate

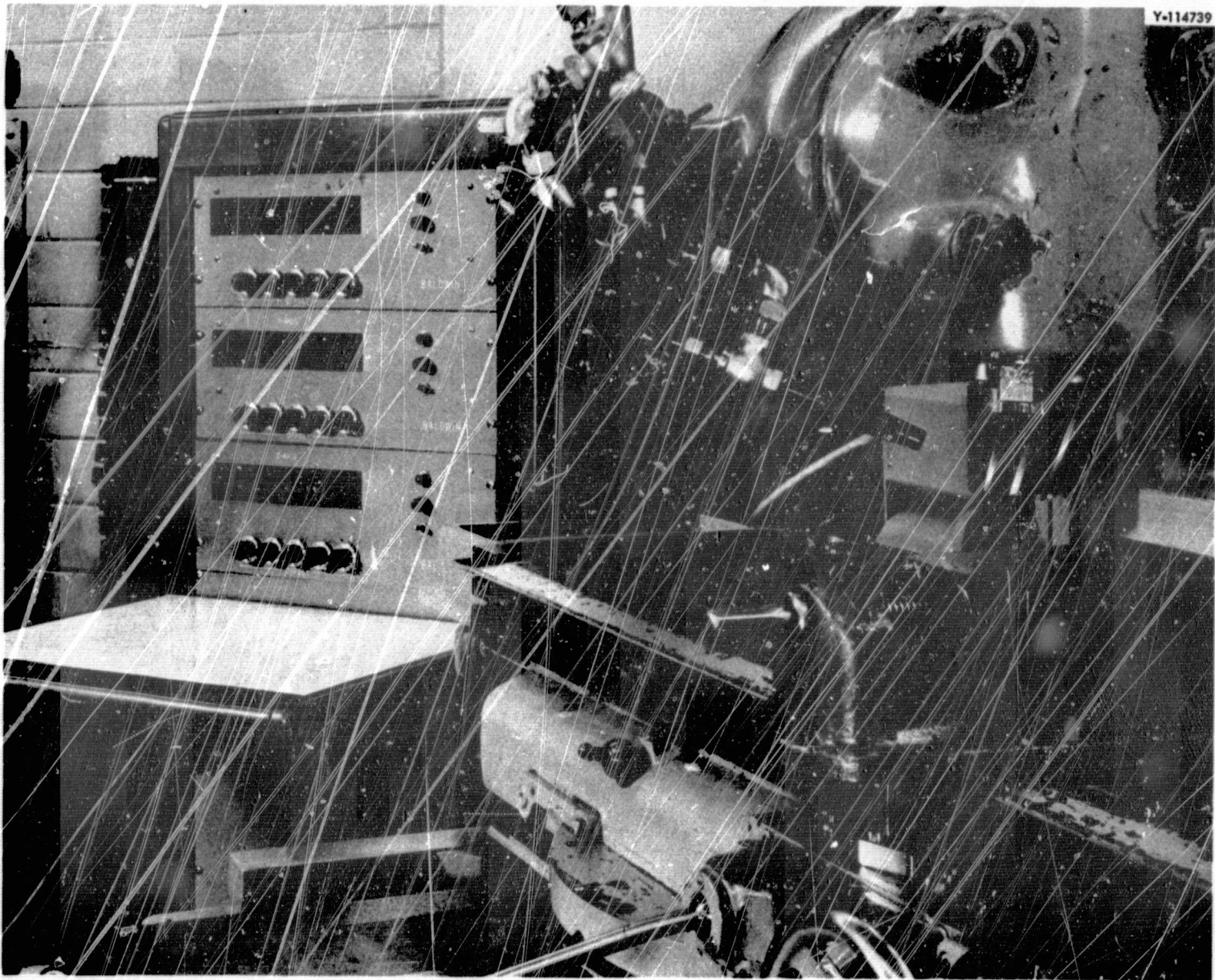


Fig. 1. Tape-Controlled Milling Operation in Fabrication of S-4 Experimental Hardware.



containing the required amount of  $^{32}\text{P}$  on the surface of each disc. The liquid was spread evenly over the entire source area and allowed to dry, forming a hard silicate layer in which the isotope was evenly distributed. Although satisfactory sources were made by this method, it was found that the silicate layer was prone to cracking and flaking in vacuum if it became moist, as could happen through a drop in the temperature of the experimental device to below the dew point of the contained air. The design of the source layer was therefore changed.

Experiments with materials such as sauer eisen and polyvinyl alcohol as substitutes for the potassium silicate were unsatisfactory. No material was found which would adhere well to the platinum surface and withstand radiation, vibration, and humidity tests and at the same time allow a reasonably homogeneous distribution of the isotope. In consequence, a new approach was used which made distribution of the isotope independent of the formation of a durable surface layer.

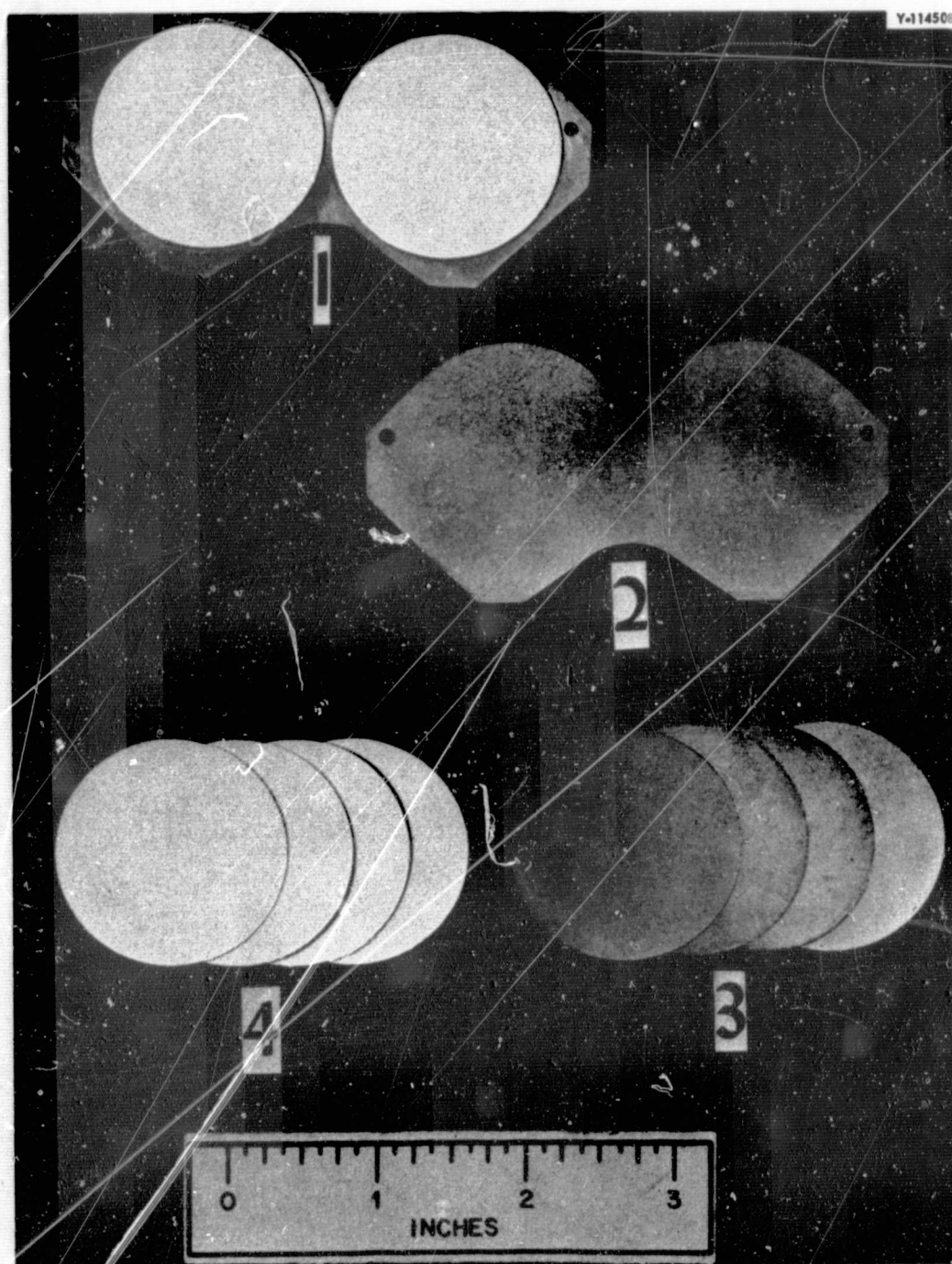


Fig. 2. Revised S-4 Experiment  $^{32}\text{P}$  Source-Plate Assembly: (1) Complete Source-Plate Assembly Ready for  $^{32}\text{P}$  Application; (2) Aluminum Support Plate; (3) Platinum Source-Plaque Backing Foils; (4) Filter Paper Discs.

The final design of the source-plate assemblies is shown in Fig. 2. A layer of epoxy resin (Epon 828 with TETA catalyst) is applied to the platinum disc and allowed to become tacky. A 4-cm disc of filter paper is then applied to this surface. The epoxy resin thus cements the paper in place without impregnating it to any significant degree. After the epoxy layer has cured completely, the required amount of isotope is applied to the paper as aqueous solution in that volume required to just saturate the paper (Fig. 3). As the paper dries, the isotope is left distributed evenly within the fiber matrix of the paper in the form of tiny trapped crystals. When the filter paper has dried completely, the amount of epoxy resin required to just saturate the paper is added and allowed to cure. The isotope is thus distributed in the form of very small crystals within a layer of hard epoxy resin. Qualification testing showed that these sources are extremely durable, and the method produces a satisfactorily homogeneous distribution of isotope over the surface area (Fig. 4).

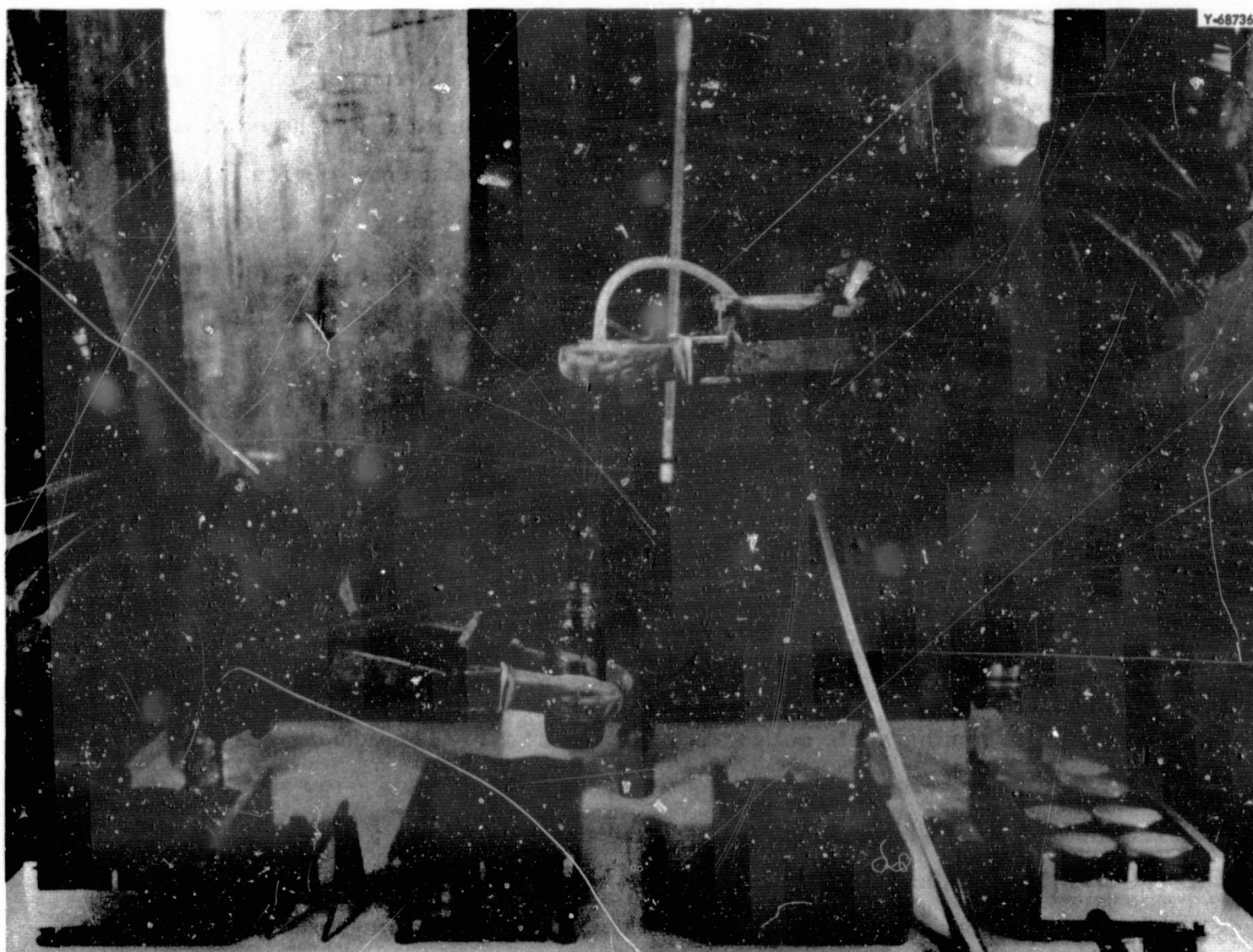


Fig. 3. Pipetting  $^{32}\text{P}$  Solution in Hot Cell During Final Source-Plate Preparation. A measured volume of solution is applied to the center of each of the source discs on each of the plate assemblies.



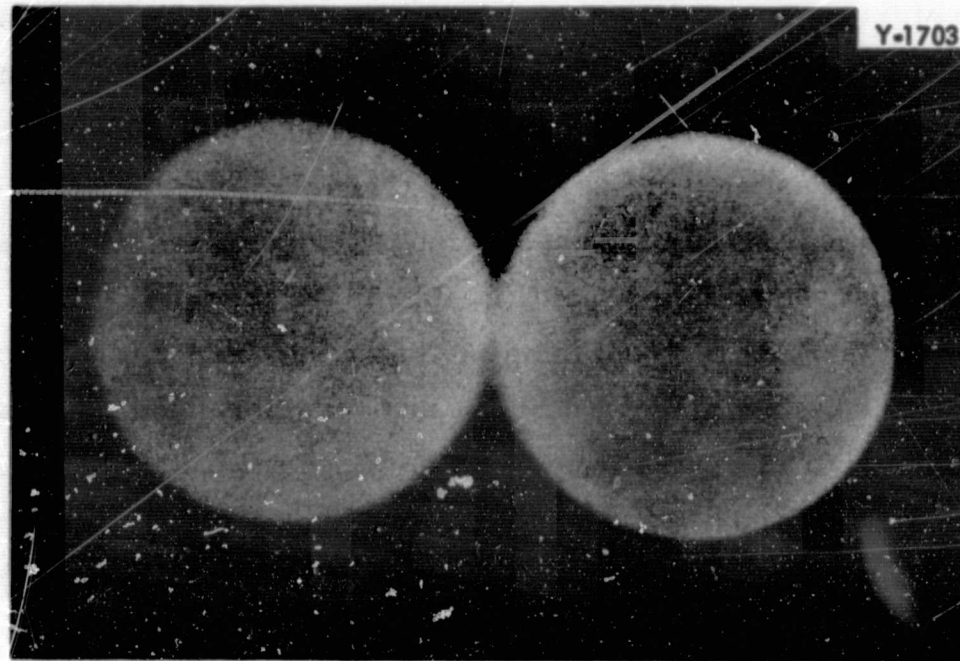


Fig. 4. Autoradiograph of Typical  $^{32}\text{P}$  Source Plate. This method was used to test each source for inhomogeneities in  $^{32}\text{P}$  distribution.

### B. Instrumentation

Although no major changes were made in the design of the instrumentation packages described previously (ORNL-TM-940), two additions were made. Tests showed that the color film strips would become fogged because of stray radiation within the experimental device if they were kept in the device too long. To preclude this possibility a platinum shield was designed which also served as the film-strip holder. This shield is shown on a completed instrumentation package in Fig. 5. The plate and screw in the center of the shield are the closure for the hole through which the film strips are inserted. The close tolerances within the shield made it necessary to fabricate a special punch and die for cutting the unexposed film into strips of the required dimensions. The other addition consisted simply of applying "TemPlet" (Wm. Wahl Co., No. 240 and No. 440) maximum-temperature indicators to the outside surface of the package to provide additional evidence in the event difficulties which could be due to high temperature within the experimental devices were encountered during the actual experiment.

Assembly of the flight-qualified instrumentation packages required the use of micro techniques in a dust-free environment (Fig. 6). An assembly with the electrical and optical parts mounted on the printed circuit board prior to potting is shown in Fig. 7. The comprehensive tests made on each flight-qualified package included electrical, mechanical, and x-ray checks in addition to those required for functional verification and qualification tests. Radiographs were used to measure the positions of the microcoulometer gaps before and after operation (Fig. 8). The thermo switches were found to differ from each other in exact switching temperatures, and it was necessary to run complete increasing and decreasing temperature profiles for each device. The pre- and postflight profiles for the instrumentation package used for the flight portion of the GT-3 S-4 experiment are shown in Fig. 9.



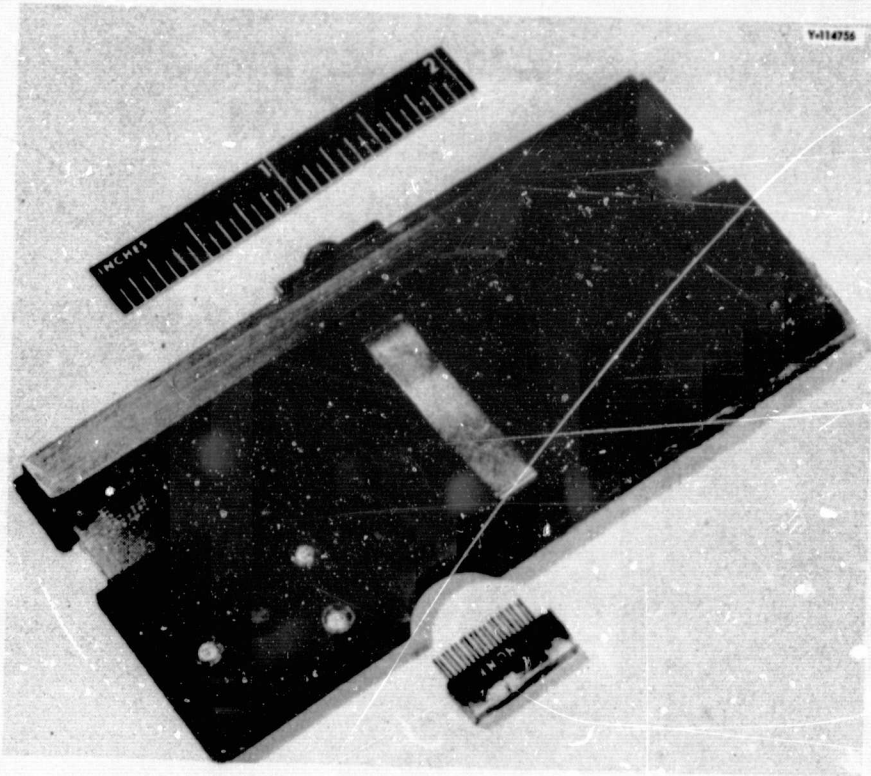


**Fig. 5. Complete S-4 Instrumentation Package.** The platinum shield for the film strips is at the top of the device; the screw and plate constitute the closure for the opening through which the films are loaded. The cavities on either side of the device contain fluoroglass dosimeter blocks. The metal strip down the center of the instrument is the event marker switch. The plug below the device is used to turn the instrument on and off.

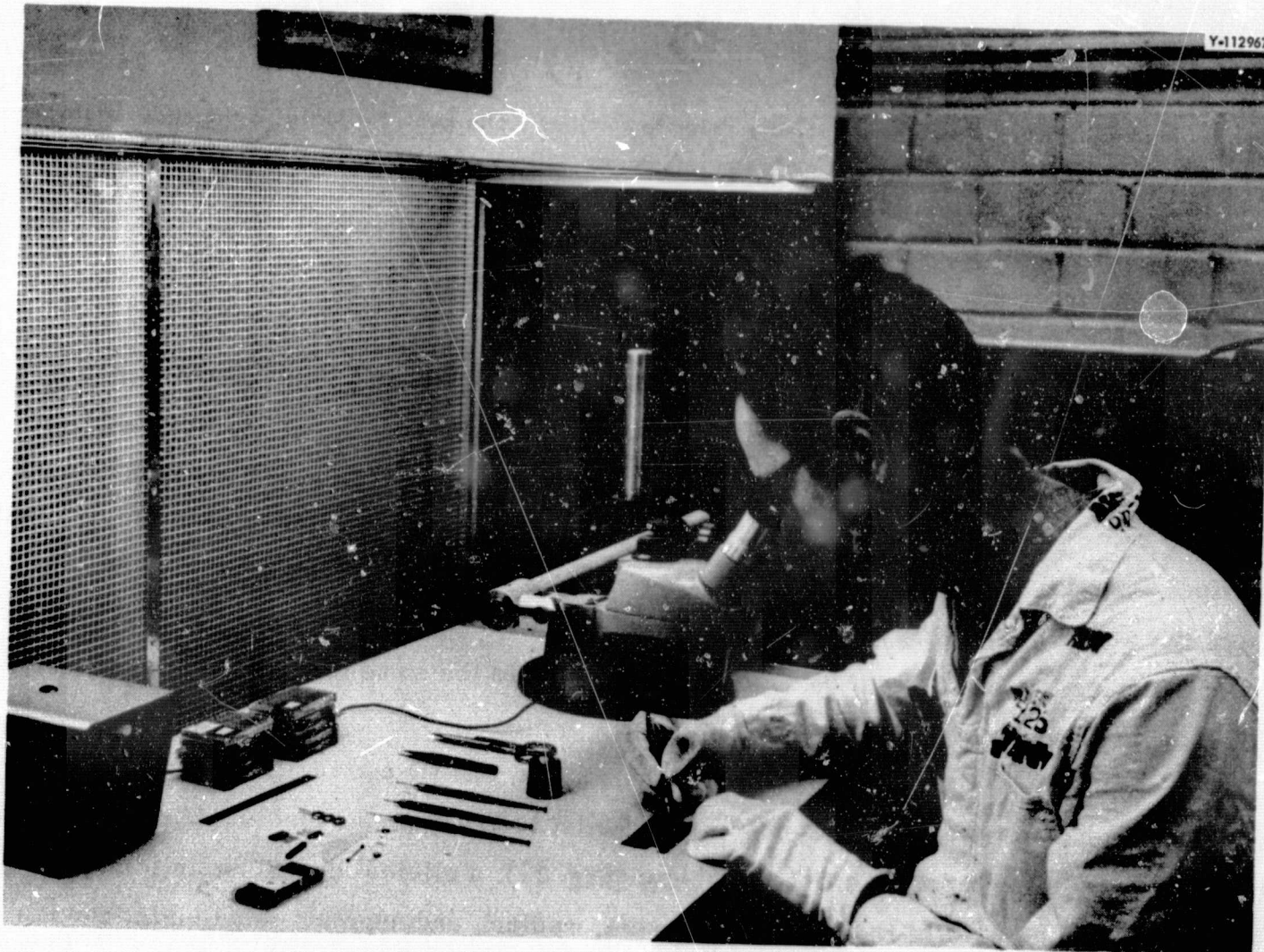


**Fig. 6. Micro-Soldering Instrumentation Package at Special "Clean" Bench.**



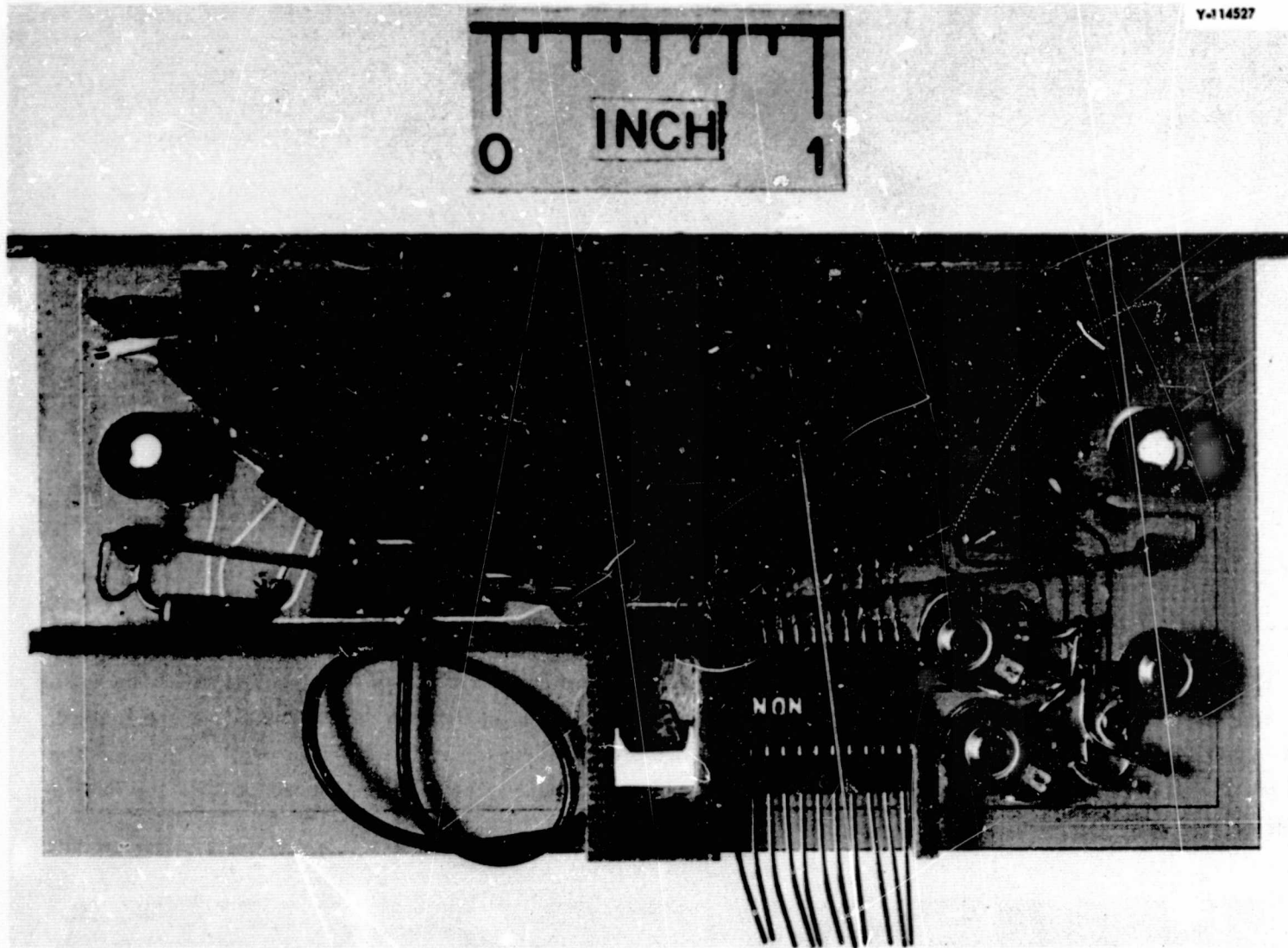


**Fig. 7. Instrumentation Package Assembly Prior to Potting.** The gap is visible in the microcoulometer at lower left. The open rectangular area at lower left is the battery compartment.

### C. Supporting Equipment

The launch-site assembly and laboratory trailer was completed with the addition of a new welding machine and a temperature-controlled cabinet. The final arrangement of the shop compartment is shown in Fig. 10. The welding current from the new machine can be decreased continuously to zero, a feature which greatly facilitated making the vacuum-tight field weld required during final assembly of the experimental devices. The temperature-controlled cabinet (located on top of the welding machine) will maintain temperatures above or below ambient. It provided a means of exposing the ground control experimental device to the same temperatures reported for the GT-3 cabin during the flight.

Three portable field kits of equipment were assembled, one for use on the prime recovery vessel and one each to cover the first- and second-orbit recovery area vessels. These kits each consisted of four units: a portable CO<sub>2</sub> incubator (Fig. 11); a clinical centrifuge in transport case; a case containing all of the sterile glassware, medium, and supplies required for making the necessary tissue cultures from the flight blood samples (Fig. 12); and a case containing a

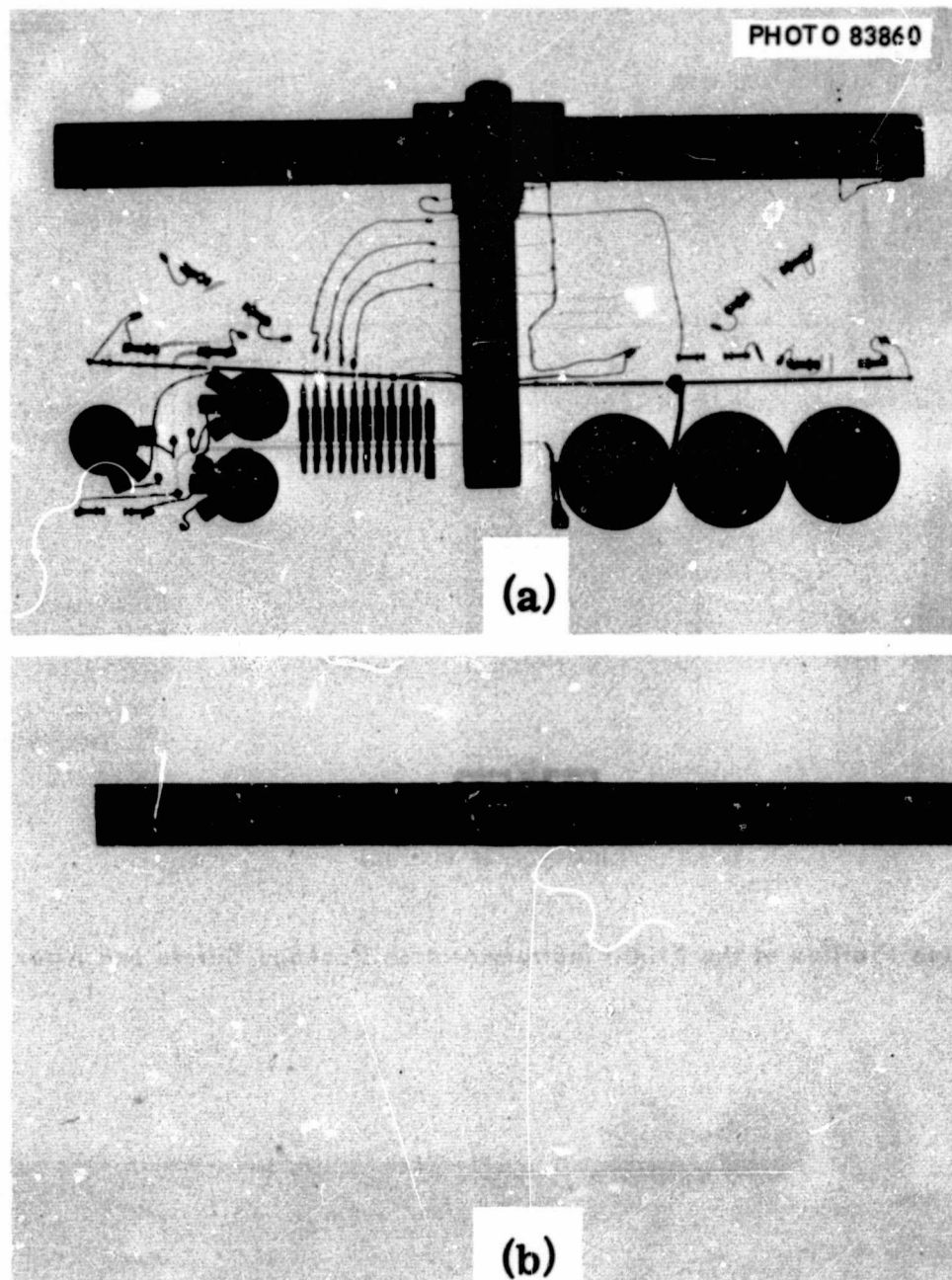


**Fig. 8. X-Ray Photographs of the Flight Instrumentation Package Which Were Used to Measure Microcoulometer Gap Position and Thus Calibrate Instrument.**

radiation survey meter, lead-shielded transportation casket for the recovered flight experimental device, and the tools necessary for opening the recovered device (Fig. 13). Although some of the items included in these kits would generally be available in a ship's sick bay, the kits' completeness made it unnecessary to depend on them.

#### **D. Dosimetry**

Complete and accurate characterization of the radiation received by the blood samples was considered an absolute requirement for the S-4 experiment. Although the short penetrating range of the  $^{32}\text{P}$   $\beta$  particles ( $R_{\text{max}} \approx 800 \text{ mg cm}^{-2}$ ) minimized shielding problems, it also complicated dosimetry somewhat. Estimation of the absolute average doses absorbed by the blood

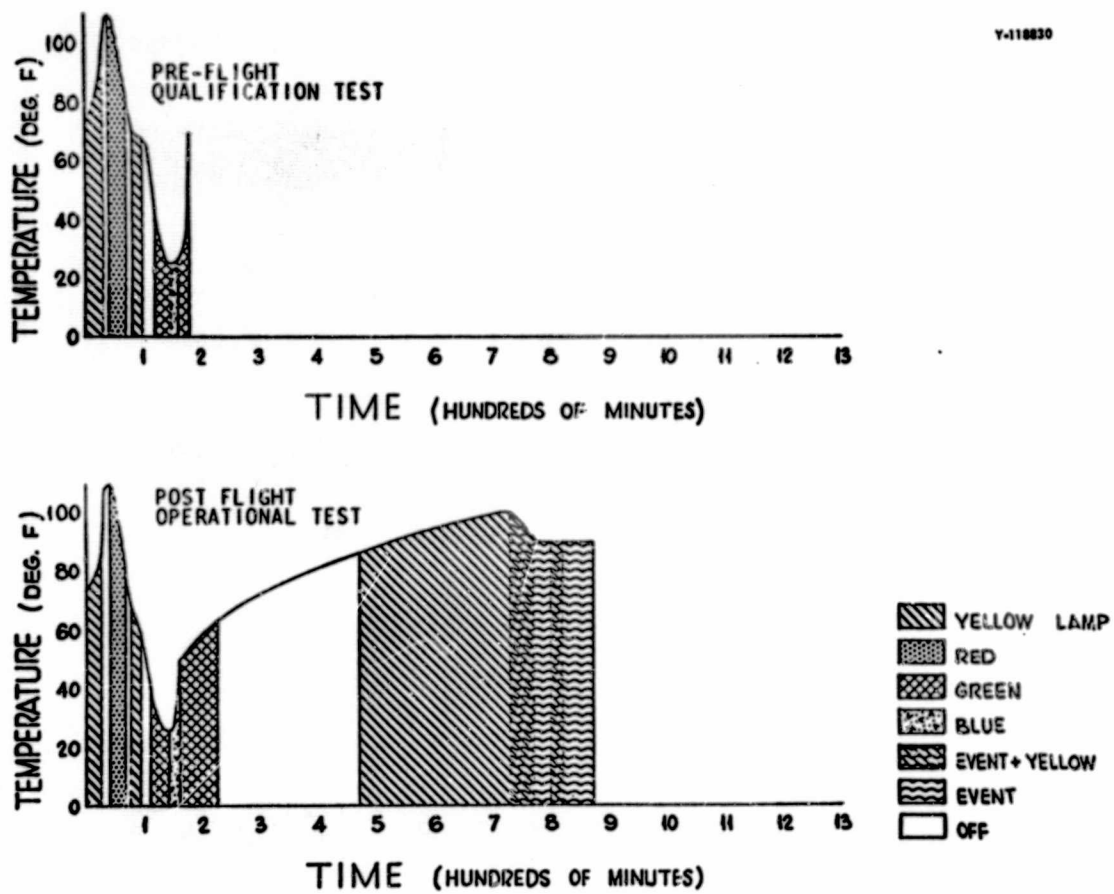


Fig. 9. Temperature Profiles of the Flight Instrumentation Package Before and After the GT-3 Flight.

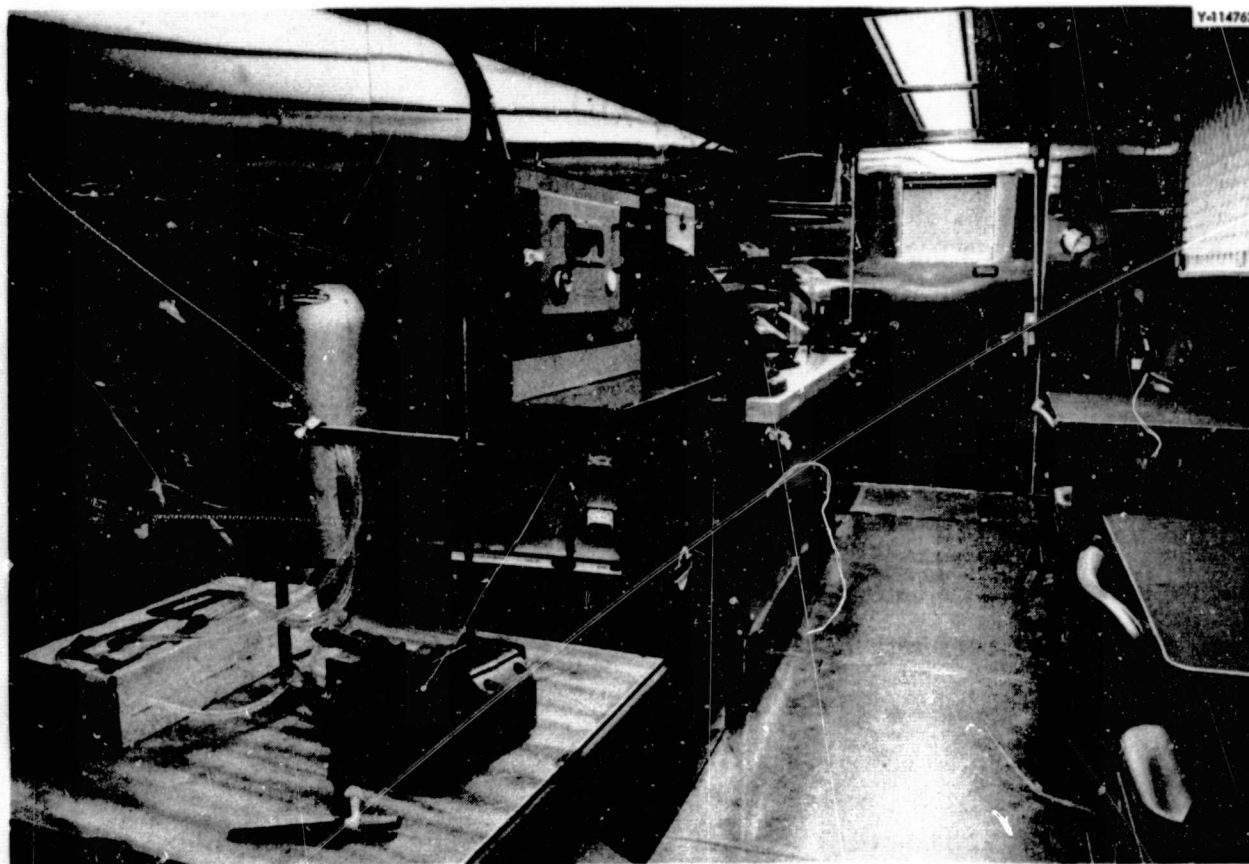
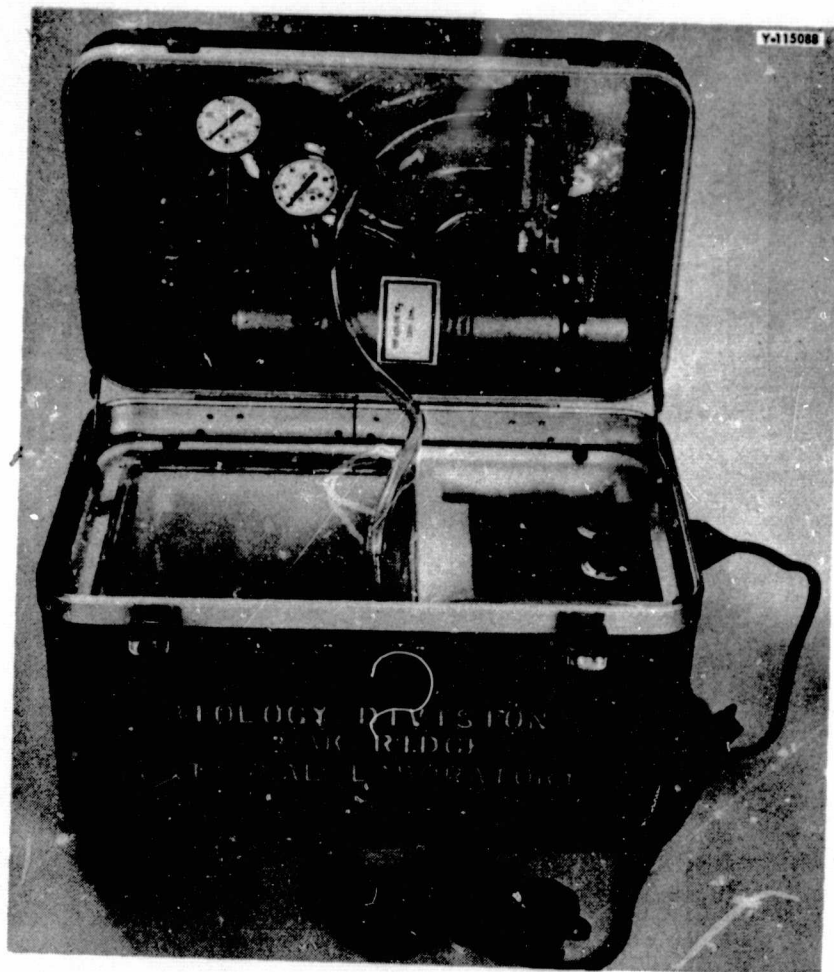
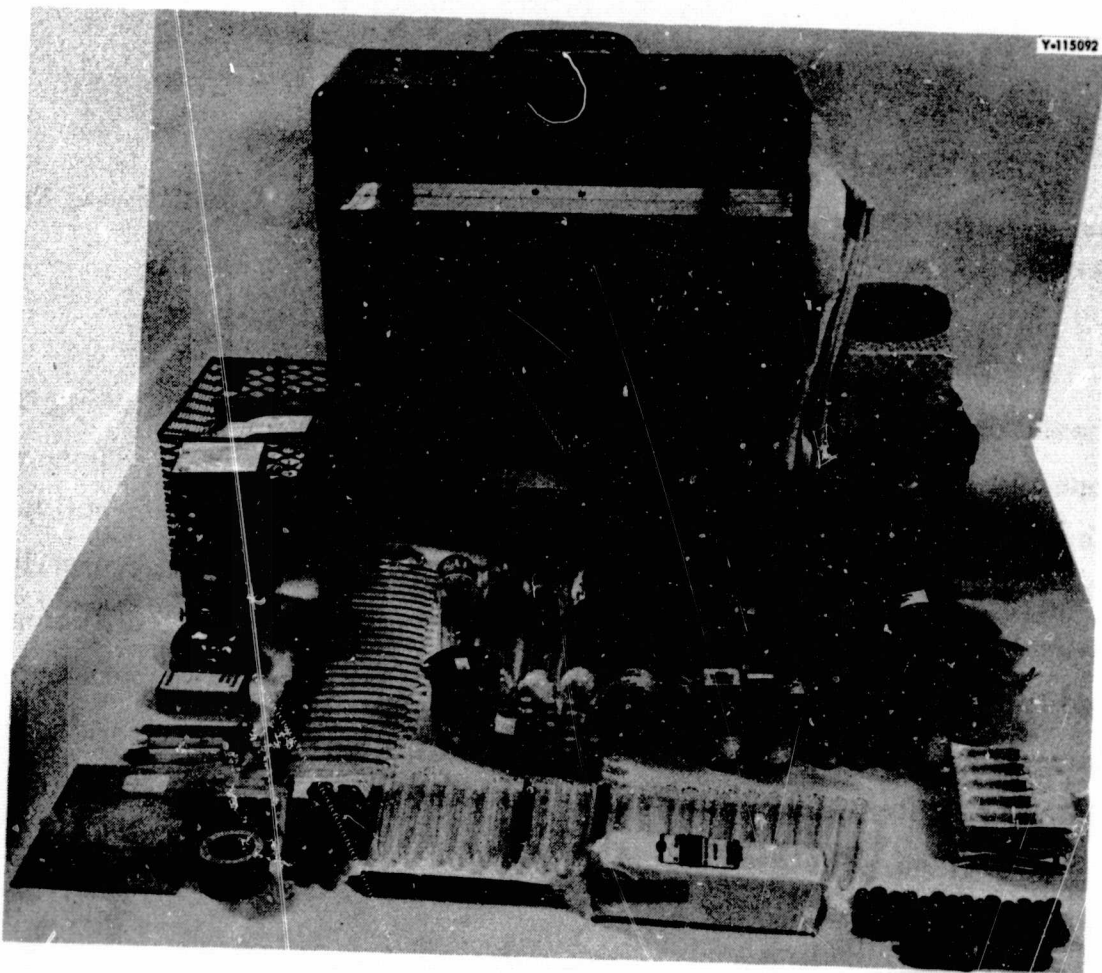


Fig. 10. View of the Final Arrangement of the Shop Area of the Trailer Used at the Launch Site. The new welding machine is on the left, with the controlled-temperature device used to provide temperature control of the ground control device located on top.





**Fig. 11. Portable Incubator with 5% CO<sub>2</sub> Supply Which Was Used on Board the Recovery Vessels.**



**Fig. 12. Laboratory Supply Kit Used to Process Flight Blood Samples Aboard Recovery Vessel. All materials and supplies necessary for preparation of the sterile tissue cultures, fixation, and cytological preparation are included.**

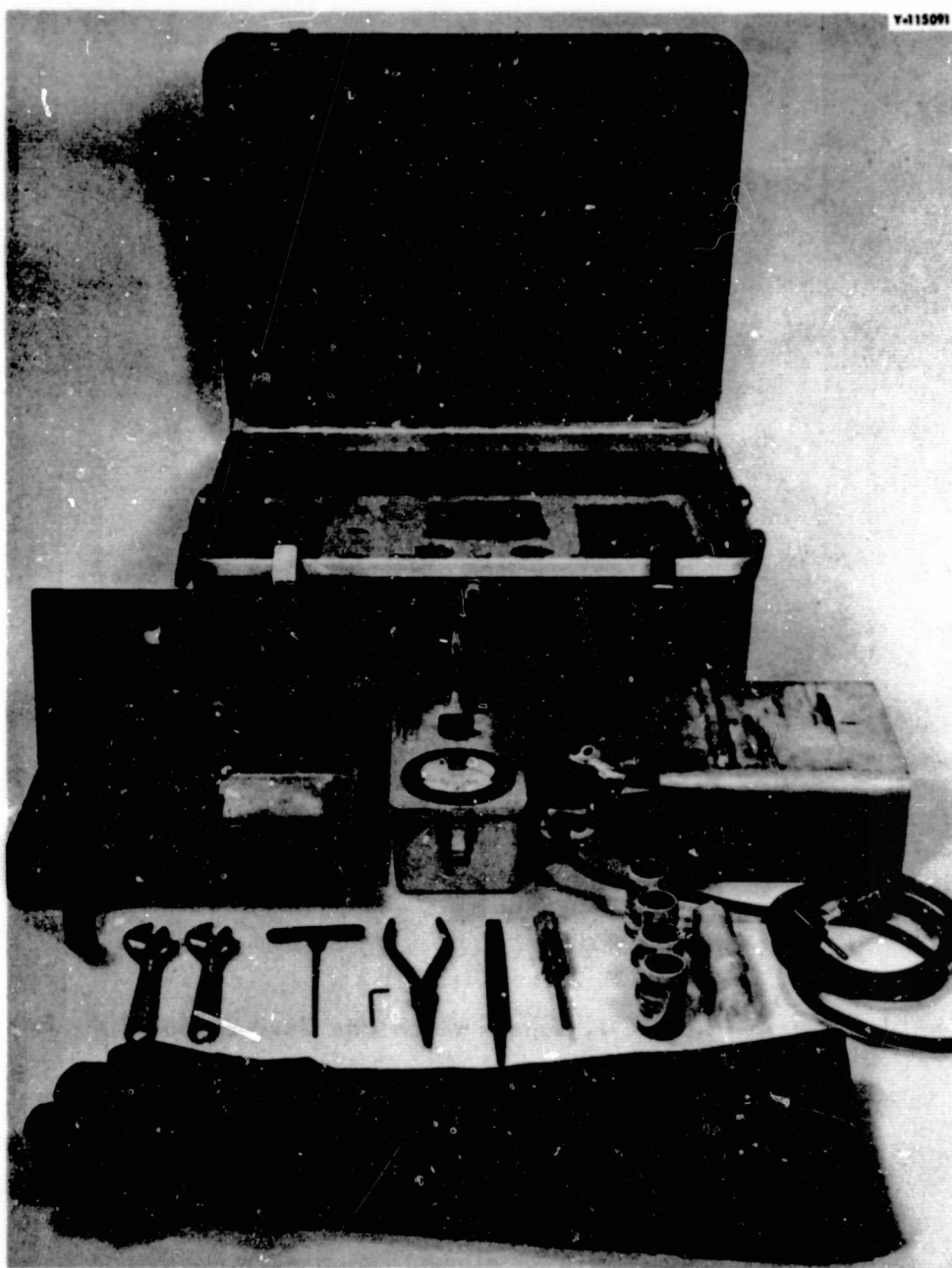


**Fig. 13. Recovery Area Kit for Cutting Open the Recovered S-4 Experimental Device, Radiation Monitoring, and Transportation of the Device Components.**

samples was based on theoretical calculation from nominal source strength, using the empirical formula developed by Loevinger<sup>1</sup> for dose distribution around  $^{32}\text{P}$  sources. These estimates were checked by experimental estimation from calibrated thin plates of silver-activated fluoroglass and by means of Fricke solution dosimetry, which not only measures dose accurately but also provides a reasonable simulation of the blood samples. The silver-activated fluoroglass rod dosimeters used to monitor the doses to the blood samples during actual experiments and the fluoroglass block dosimeters used in the instrumentation packages were calibrated in reference to these absolute dose determinations. Finally, the bremsstrahlung spectrum of the experimental devices was characterized. The geometrical relationships pertaining to dosimetry within the experimental devices are shown in Fig. 14.

<sup>1</sup>R. Loevinger, *Science* 112, 530-31 (1950); R. Loevinger, E. M. Japha, and G. L. Brownell, in *Radiation Dosimetry* (G. J. Hine and G. L. Brownell, eds.), pp. 693-799, Academic Press, New York, 1956.

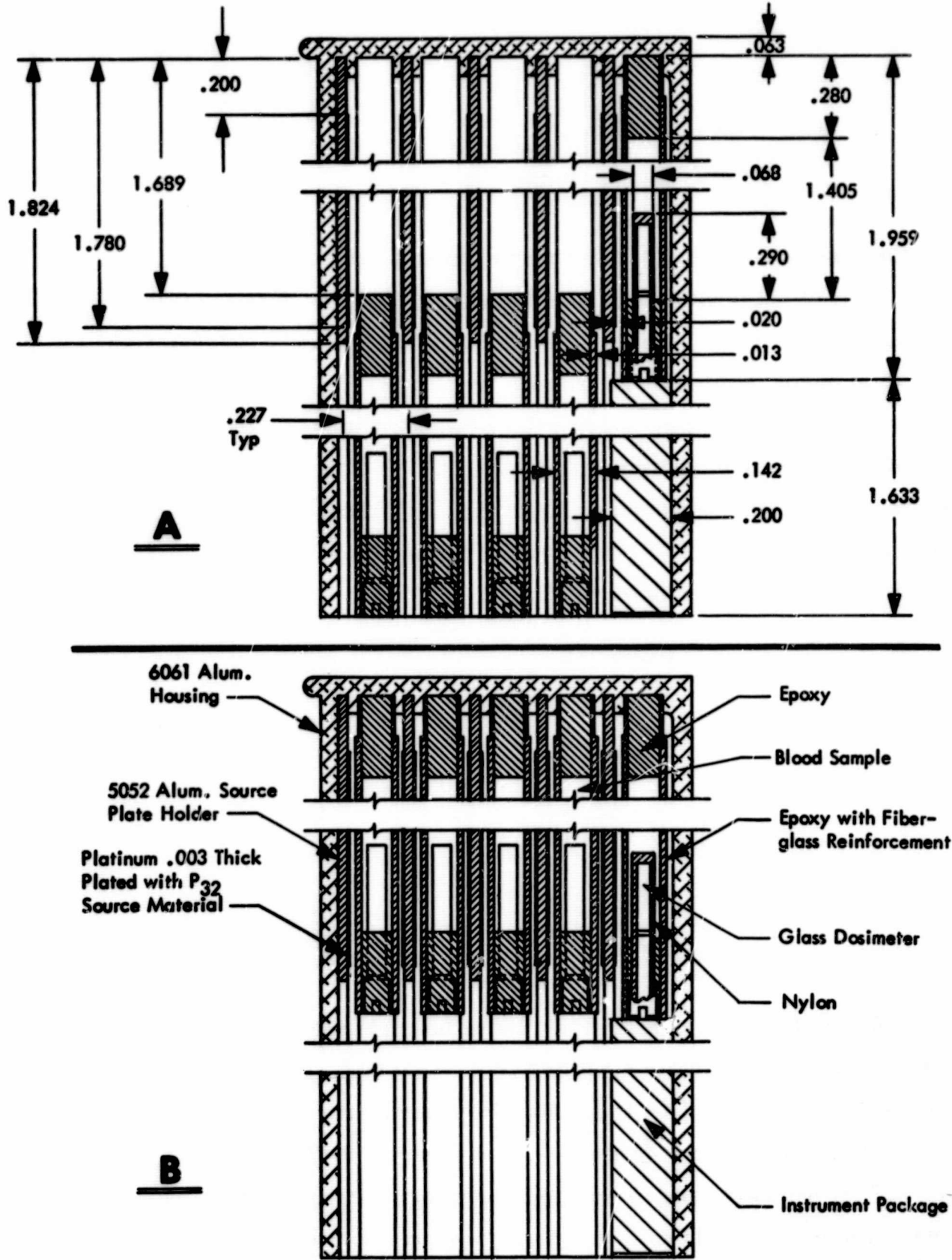


Fig. 14. Cross-Sectional Drawing Showing Relation of Source Plaques and Blood Samples when the S-4 Experimental Device Is in the "Nonirradiating" (A) and the "Irradiating" (B) Modes.

**Theoretical.** — Loevinger's empirical formula for dose-rate distribution around a point source of  $^{32}\text{P}$   $\beta$  particles, derived from extrapolation chamber ionization measurements of plane sources is

$$j(r) = \begin{cases} \frac{k}{\nu\rho r^2}, & r \leq 1/\nu\rho, \\ \frac{ke^{(1-\nu\rho r)}}{\nu\rho r}, & r > 1/\nu\rho, \end{cases} \quad (1)$$

where  $j(r)$  is the dose rate at a distance  $r$  from the point source,  $\nu$  the absorption coefficient of the exponential part of the plane source attenuation curves,  $\rho$  the density of the *homogeneous* material surrounding the source, and  $k$  the normalizing constant to be determined by the requirement that the total energy absorbed per sec in a very large sphere must be just equal to the product of the average  $\beta$ -ray energy and the  $\beta$ -ray emission per sec from the source.

The dose-rate-distribution function  $R(x)$  at a distance  $x$  from an infinite plane slab source of finite thickness in which  $^{32}\text{P}$  nuclei are uniformly distributed may be derived from Eq. (1); application of Eq. (1) to the case of the S-4 experimental device gives the dose rate  $R(t)$  at a depth of  $t$  from the surface of the blood sample as:

$$R(t) = \frac{0.694\nu\rho\Omega}{6} \times 1.52g(t) \text{ Mev sec}^{-1} \text{ cm}^{-2}, \quad (2)$$

where

$$g(t) = \begin{cases} e^{-0.957\rho t}, & \text{for } t < \frac{0.35}{\rho} \text{ (mm)}, \\ 0.987e^{-0.92\rho t}, & \text{for } t \geq \frac{0.35}{\rho} \text{ (mm)}, \end{cases}$$

values of  $E_\beta = 0.694 \text{ Mev}$  and  $\nu = 9.2 \text{ cm}^2 \text{ g}^{-1}$  have been assumed, and  $\Omega$  is surface density of beta rays of the  $^{32}\text{P}$  source in disintegrations per sec per  $\text{cm}^2$ . Here the complicated initial part of the attenuation in the range of  $t < 0.35/\rho$  has been approximated by the exponential function  $e^{-0.957\rho t}$ , which fits the rigorous function with an accuracy better than 0.5%.

Conversion from the units used in Eq. (2) to practical units is straightforward. For example, the dose rate  $r(t)$  in units of  $\text{rads hr}^{-1}$  at a depth of  $t$  mm in blood is:

$$r(t) = 3.43 g(t) \text{ rads hr}^{-1} \mu\text{C}^{-1} \text{ cm}^2, \quad (3)$$

where

$$g(t) = \begin{cases} e^{-0.957t}, & \text{for } t < 0.35 \text{ mm}, \\ 0.987e^{-0.92t}, & \text{for } t \geq 0.35 \text{ mm}. \end{cases}$$



The relative depth-dose curve calculated from this equation is shown in Fig. 15.

Since Loevinger's equation is valid only for homogeneous medium surrounding a  $^{32}\text{P}$  source, and since the S-4 sources are backed by platinum foil, an empirical correction for the actual S-4 sources is needed. It should be noted that because the  $^{32}\text{P}$  sources are backed by a high-Z material like platinum, backscattering only increases the dose rate inside the blood-sample chamber and does not appreciably change the  $\beta$ -particle energy distribution.

Since the blood samples are irradiated between pairs of  $^{32}\text{P}$  source plaques, the actual depth-dose curve for the 3-mm-thick blood samples is the sum of the doses at depth  $t$  and at  $(3-t)$ . The incident  $\beta$  radiation is partially absorbed by the thin ( $5.5 \times 10^{-2} \text{ g cm}^{-2}$ ) epoxy-fiber-glass window of the blood-sample holder on each side of the blood sample. After normalizing the value at either surface of the blood sample itself to unity, we have the curve shown in Fig. 16. The ratio of maximum to minimum dose rate is 2.13.

Equation (4) can be used to calculate the average dose rate,  $R_{\text{blood}}$ , for the 3-mm-thick blood samples inserted, for example between a pair of 1.25 mC  $^{32}\text{P}$  plaques. The average dose rate due to  $100 \mu\text{C cm}^{-2}$  activity of the 4-cm-diameter discs must be corrected for the platinum backscattering effect and for the thickness of the window of the blood-sample chamber, both determined experimentally:

$$R_{\text{blood}} = 100 \times 2 \times 1.23 \times 3.43 \times 1/3 \times \int_{0.55}^{3.55} g(t) dt \quad (4)$$

$$= 283 \text{ rads per hr.}$$

The value 1.23 is the empirical correction for backscatter. This value was derived as explained below.

**Experimental.** — In order to measure absolute dose rates inside the blood-sample chambers, thin fluoroglass plates,  $8 \times 8 \times 0.14 \text{ mm}$ , were fabricated. A blood-sample chamber was filled with a stack of 31 discs cut from polyethylene sheet about  $10 \text{ mg cm}^{-2}$  thick in order to simulate a blood sample. A single  $^{32}\text{P}$   $\beta$  source was used to irradiate this polyethylene "phantom" from one side of the blood-sample holder. Counting from the side nearest to the  $^{32}\text{P}$  plaque, the second, tenth, twentieth, and thirtieth sheets had an  $8 \times 8 \text{ mm}$  hole cut in the center to accommodate a fluoroglass plate. In order to match the thickness of the plates ( $37 \text{ mg cm}^{-2}$ ) to that of the polyethylene sheets, the next disc on either side of the fluoroglass plate also had an  $8 \times 8 \text{ mm}$  hole. The exposed fluoroglass was read with a Toshiba Type B3 fluorometer. To convert from fluoroglass plate midpoint to the polyethylene depth, the plate was considered to be an 0.37 mm polyethylene sheet.

The major difficulty in the thin-plate method was calibration of the fluorescence readings in terms of polyethylene dose. If the plate were infinitely thin, the calibration could be made by applying the Bragg-Gray principle:

$$D_{\text{poly}} = \frac{(S_m)_{\text{poly}}}{(S_m)_{\text{glass}}} D_{\text{glass}}, \quad (5)$$



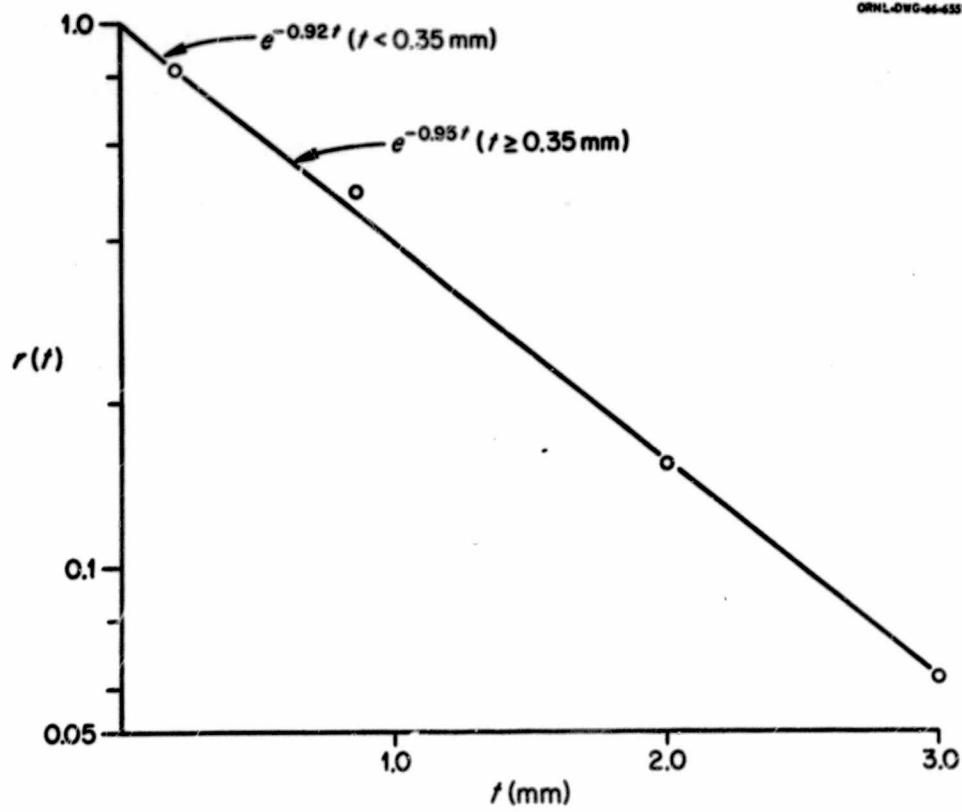


Fig. 15. Depth-Dose Curve for Polyethylene Phantom Exposed to a Single  $^{32}\text{P}$  Source. The line is the theoretical curve; points are the experimentally measured values at various depths within the phantom. Abscissa: depth in mm. Ordinate: logarithm of relative dose.

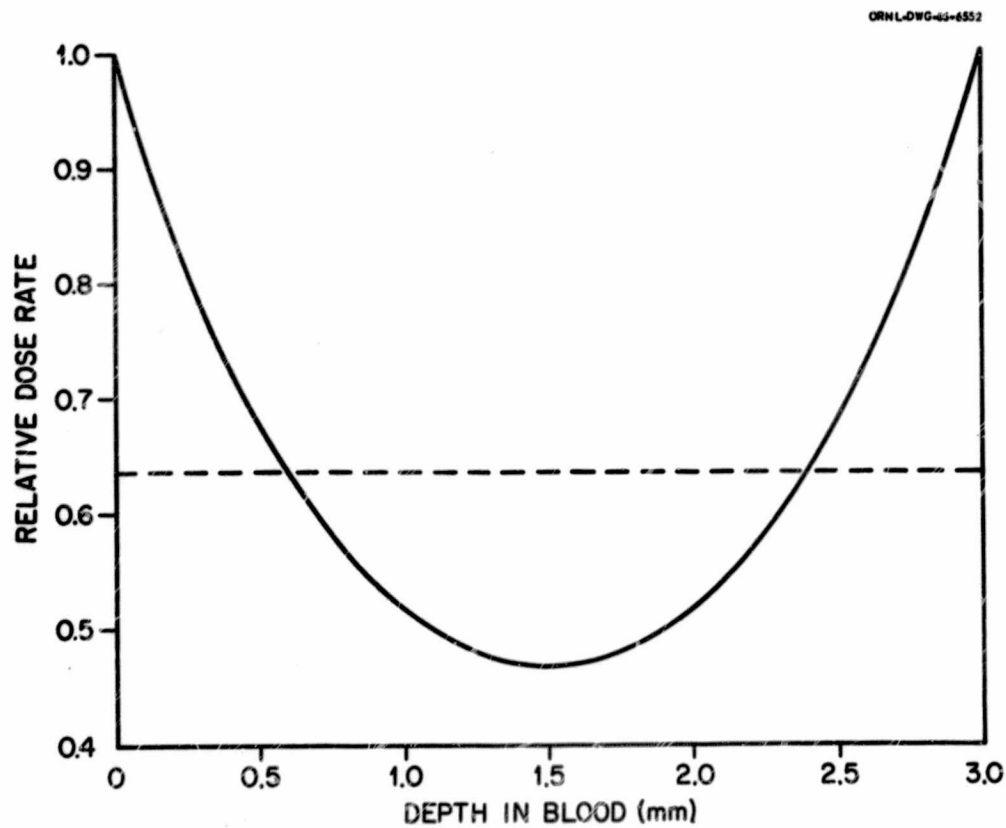


Fig. 16. Depth-Dose Curve for Blood Sample Irradiated by a  $^{32}\text{P}$  Plaque on Each Side. Dotted line is dose rate integrated over the entire sample depth. Abscissa: depth in sample in mm. Ordinate: dose rate in relative units.

where  $D_{\text{poly}}$  and  $D_{\text{glass}}$  are the doses in polyethylene and glass and  $(S_m)_{\text{poly}}$  and  $(S_m)_{\text{glass}}$  are the average mass-stopping powers of these substances. This is not rigorously valid, however, because the fluoroglass plate is actually  $37 \text{ mg cm}^{-2}$  thick. The plate absorbs about 25% of the incident  $^{32}\text{P}$   $\beta$  particles. Furthermore, electron scattering at the glass-polyethylene interface may not be negligible. It is well known that the depth-dose curve for monoenergetic electrons changes shape with a change in atomic number of the material exposed. This complexity can be avoided if the  $\beta$  radiation is simulated with high-energy  $\gamma$  radiation. Because of the production of Compton electrons, the polyethylene sheets exposed to a  $\gamma$ -ray beam can be considered as a source of a roughly monodirectional electron beam, and the Compton electrons originating in the thin fluoroglass plates lose only a very small fraction of their total energy within the plates. In other words, if a fluoroglass plate at a certain depth in the stack of polyethylene sheets exposed to  $^{32}\text{P}$   $\beta$  particles gives a fluorescence yield equal to that of one exposed in the same way to  $\gamma$  rays, the dose in the polyethylene around the plate must be equal for both the  $\beta$  and the  $\gamma$  radiation. Obviously, measurement of the dose in  $\gamma$ -irradiated polyethylene may be simplified by substitution of a calibrated ionization chamber.

The method described was carried out using a  $^{137}\text{Cs}$   $\gamma$  beam, the intensity of which was calibrated with a Victoreen condenser r meter previously calibrated for  $^{137}\text{Cs}$   $\gamma$  rays at the National Bureau of Standards. Typical values for both  $^{60}\text{Co}$  and  $^{137}\text{Cs}$  are given in Table 1. The inverse of the specific response ( $A/r$ ) for these exposures gives the conversion factor, 3.37, from fluoroglass-plate reading to polyethylene dose in rads. Using this conversion factor, the readings of the thin fluoroglass plates at the four different depths in the polyethylene blood-sample phantom exposed to a 2.5 mC  $^{32}\text{P}$  source were converted to depth doses in rads and

Table 1. Calibration of Fluorescence Yield of Rod and Thin-Plate Fluoroglass Dosimeters Given Known Exposures to  $^{137}\text{Cs}$  and  $^{60}\text{Co}$   $\gamma$  Rays

Dosimeter Type	Source	Standard	Exposure (r)	Specific Response <sup>a</sup> ( $\mu\text{A/r}$ )	Exposure Rate (r/min)
1 x 6 mm rod	$^{60}\text{Co}$	NBS <sup>b</sup>	100	$0.504 \pm 0.027$	6.69
1 x 6 mm rod	$^{60}\text{Co}$	NBS	300	$0.513 \pm 0.007$	6.69
1 x 6 mm rod	$^{137}\text{Cs}$	Victoreen <sup>c</sup>	190	$0.500 \pm 0.005$	2.47
1 x 6 mm rod	$^{137}\text{Cs}$	Victoreen	326	$0.517 \pm 0.014$	2.47
8 x 8 x 0.14 mm plate	$^{137}\text{Cs}$	Victoreen	326	$0.297 \pm 0.028$	2.47

<sup>a</sup>Readings made with a Toshiba fluorometer, type B3. The sensitivity of the fluorometer was slightly different for rods at 300 and 326 r and for those at 100 and 190 r because a scale change was necessary.

<sup>b</sup>Rods exposed to  $^{60}\text{Co}$   $\gamma$  rays at the National Bureau of Standards.

<sup>c</sup>Exposure measured with a 2.5 r Victoreen chamber calibrated against a  $^{137}\text{Cs}$   $\gamma$ -ray beam at the National Bureau of Standards.

compared with the theoretical values. As shown in Table 2, Loevinger's equation fits very well the experimental dose-distribution in absolute units.

The experimentally determined depth doses allow a check on the accuracy of the preparation of the  $^{32}\text{P}$  source plaques with the desired absolute activity. The initial source activity was intended to be 2.5 mC per plaque. The activity of the original  $^{32}\text{P}$  solutions used in source-plate preparation was checked by means of an end-window gas-filled  $\beta$  proportional counter previously calibrated against a  $^{47}\text{T}$  counter originally calibrated against standards prepared by the National Bureau of Standards. The doses measured by means of the fluoroglass plates were all normalized to the first day by correcting for  $^{32}\text{P}$  decay. The ratio of 0.977 of the sum of the experimental depth doses to that of the theoretical values indicates satisfactory agreement. The ratio of 0.977 was then taken (for convenience) to be the ratio of the actual activity of the  $^{32}\text{P}$  plaques to the nominal activity. Thus the estimated average dose to the blood sample exposed to these 2.5 mC plaques for 20 min should be equal to the theoretical value, 188.7 rads, times 0.977, or 184.5 rads.

Table 2. Reading of Fluoroglass Plates in a Polyethylene Phantom Exposed in a Blood-Sample Chamber to a 2.5-m.C  $^{32}\text{P}$  Source

Depth <sup>a</sup> (mm)	Exposure Time (min)	Fluorescence ( $\mu\text{A}$ )	$\mu\text{A}/20\text{ min}^b$	Absorbed Dose (rads/20 min) <sup>c</sup>	
				Exptl.	Theoret. <sup>d</sup>
0.21	125	98.2	60.0		
	103	82.4	65.7	218 $\pm$ 14	224
	103	85.5	68.3		
1.06	125	49	29.9		
	103	38.1	30.4	105 $\pm$ 7	104
	103	42.2	33.7		
2.01	125	20.3	12.4		
	103	14.8	11.4	40.8 $\pm$ 1.5	43
	103				
2.96	125	7.2	4.4		
	103	6.01	4.8	15.9 $\pm$ 1.0	18.2
	103	6.21	5.0		
			Sum	379.7	389.2
			Ratio	0.977	1.000

<sup>a</sup>Midpoints of glass plates, 37 mg/cm<sup>2</sup> thick. Each glass plate was treated as if it were a polyethylene sheet 0.37 mm thick.

<sup>b</sup>After decay correction.

<sup>c</sup>0.297  $\mu\text{A}/\text{rad}$ -polyethylene was the conversion factor calibrated by  $^{137}\text{Cs}$   $\gamma$  rays (see Table 1); 1 r equals 1 rad in polyethylene for  $^{137}\text{Cs}$   $\gamma$  rays.

<sup>d</sup>Correction was made for the polyethylene sheet covering the  $^{32}\text{P}$  plaque used to avoid contamination.

Table 3. Comparative Measurements by Glass Rods of Relative Intensities of  $^{32}\text{P}$  Plaques Used in the GT-3 Flight and Ground Devices and Those in Another Set Used for Calibration

$^{32}\text{P}$ Activity per Disc	Rod Reading <sup>a</sup> (rads/20 min)				Dose to Blood Sample <sup>b</sup> (rads)
	Different $^{32}\text{P}$ Plaque Sets				
	Calibration	GT3-G	GT3-F	Average	
0.625 mC	64.2	65.1	63.3	64.2	49.5
1.25 mC	129.0	121.0	123.	124.3	96.0
1.875 mC	182.0	186.0	195.0	187.7	145.0
2.5 mC	232.0	245.0	242.0	239.7	185.0

<sup>a</sup>Three bare rods encased in thin polyethylene tubes were placed at the center and 1.5 mm apart from the center in a blood chamber without other packing materials. Two sets of chambers at each  $^{32}\text{P}$  activity were used. The reading values listed are those after correction for  $^{32}\text{P}$  decay.

<sup>b</sup>Doses calculated as explained in the text from rod readings with allowance for the ratio of 0.977 (bottom of column 5, Table 2) between the fluoroglass measured dose and the theoretical value.

As a further check on nominal  $^{32}\text{P}$  source activities, accurate measurements of relative intensities of  $^{32}\text{P}$   $\beta$ -particle beams from sources of different activities were made with fluoroglass rods encased in thin polyethylene tubes to stimulate the thin wall of the dosimeter plug screws used in the experimental device. The rods were placed in the center and at 1.5 mm to either side of the center of empty blood-sample chambers. Table 3 summarizes the values obtained. Since there is no systematic variation among the three dosimeters, the average was taken as the best estimate of the relative intensity of the  $\beta$ -ray beam for a given nominal  $^{32}\text{P}$  activity. The ratio, 0.77, of 184.5 blood rads (previous paragraph) to a rod reading of 239.7 r of  $^{60}\text{Co}$   $\gamma$  exposure, obtained for the 2.5 mC plaque, was used to convert the fluoroglass readings to blood doses for the other  $^{32}\text{P}$  plaques as given in column 6 of Table 3.

Fricke solution prepared as recommended by Weiss *et al.*<sup>2</sup> was used for determinations of integrated dose to the blood samples. Optical density was measured at 305  $m\mu$  with a Beckman model D spectrometer using quartz cuvettes of 10 mm optical path length. The particular advantage of the Fricke solution for these determinations is that the irradiation of the blood sample can be simulated so easily. It is difficult to estimate, either theoretically or by means of other dosimeters, the dose-rate deviation in the radial dimension of the blood-sample chamber. The Fricke solution eliminates this difficulty.

The Fricke solution was calibrated with the same  $^{137}\text{Cs}$  beam used for the fluoroglass dosimeter calibration. The relationship between OD increase ( $A$ ) due to  $\gamma$ -ray irradiation and the dose absorbed in the Fricke solution ( $D_f$ ) is linear. Thus

$$A = kD_f, \quad (6)$$

<sup>2</sup>J. Weiss, A. O. Allen, and H. A. Schwartz, *Proc. Intern. Conf. Peaceful Uses At. Energy, Geneva, 1955* 14, 179-81 (1956).



Table 4. Doses to Blood Samples Estimated by Fricke Solution

<sup>32</sup> P Activity per Disc (mC)	OD Increase per 20-Hr Exposure <sup>a</sup>	Dose Rate in Fricke <sup>b</sup> (rads/hr)	Dose Rate to Blood Samples <sup>c</sup> (rads/hr)	Blood Dose for 20-Min Exposure
0.625	0.0975 ± 0.014	150	154	51
1.25	0.1867 ± 0.021	287	297	99
1.875	0.2744 ± 0.017	424	435	148
2.5	0.3764 ± 0.028	580	596	199

<sup>a</sup>The OD value at each dose rate is the average of ten runs. The observed OD increases were corrected for the <sup>32</sup>P decay to the initial day.

<sup>b</sup>Calculated from Eq. (8).

<sup>c</sup>Calculated from Eq. (9).

where  $k$  is a proportionality constant to be determined experimentally. Since the Victoreen chamber used to calibrate the <sup>137</sup>Cs beam is calibrated in  $r$  units,  $D_f$  must be correlated with the exposure  $R(r)$ . This may be written simply

$$D_f = 1.027 D_{H_2O} = 1.027 \times 0.975 R, \quad (7)$$

where 1.027 is the ratio of the dose in the Fricke solution (which has a specific gravity of 1.025) to that in water, and 0.975 is the conversion factor from  $r$  to rads in water at the <sup>137</sup>Cs photon energy.<sup>3</sup> Table 4 gives the experimental results for the relationship between  $R$  and  $A$ . The value obtained for the ratio  $A/R$  was  $3.24 \times 10^{-5}$ . Therefore  $K$  is  $3.25 \times 10^{-5}$ , and the conversion factor from OD increase ( $A$ ) to the absorbed dose in the Fricke solution ( $D_f$ ) is  $3.08 \times 10^4$ . One disadvantage of Fricke solution is that the value of  $K$  decreases rather rapidly with increasing LET; although it is the same for <sup>32</sup>P  $\beta$  particles and for <sup>60</sup>Co  $\gamma$  rays, it increases about 1% for <sup>137</sup>Cs  $\gamma$  rays.

Difficulty was encountered in using the Fricke solution in the blood-sample chambers because a chemical reaction with the epoxy resin used in their fabrication caused a large increase in OD. In order to reduce this effect, the exposures of Fricke solution in the blood-sample chambers to <sup>32</sup>P  $\beta$  particles were carried out at 4°C. The temperature coefficient for the OD increase due to radiation is only about -0.04% per °C. The  $\gamma$ -ray calibration was done at 24°C. Thus we have the conversion factor from the OD increase due to <sup>32</sup>P exposure,  $A_p$ , to Fricke dose,  $D_f$ , as follows:

$$D_f = 3.08 \times \frac{1}{1.01} \times 1.008 \times 10^4 A_p \quad (8)$$

$$\cong 3.08 \times 10^4 A_p.$$

However, since we are interested in the dose absorbed in blood rather than in the Fricke solution,

<sup>3</sup>National Bureau of Standards Handbook No. 78, 1961.



a further correction must be made. For simplicity, it was assumed that the blood can be reasonably accurately approximated by water. The Fricke solution used had a specific gravity of 1.025. Hence, the average dose given by the  $^{32}\text{P}$  plaque to the Fricke solution filling the blood-sample chamber should be larger than that to water or blood filling the chamber, by roughly the ratio of their specific gravities. Thus the conversion factor from the OD increase,  $A_p$ , becomes:

$$D_{\text{blood}} = 3.14 \times 10^4 A_p \text{ rads} . \quad (9)$$

Table 4 summarizes the experimental results for a typical  $^{32}\text{P}$  plaque set.

Because of  $\beta$ -particle leakage and bremsstrahlung the blood samples in the S-4 experimental device, including the control, are exposed to a very low radiation dose-rate for the entire time the device is assembled. Although small, the doses received at the control and "nonirradiating" positions are not entirely negligible. Most of the dose is from the bremsstrahlung from a platinum target (the source-plate backing) hit by  $^{32}\text{P}$   $\beta$  particles. Thus, the fluoroglass rod dosimeters within the "irradiated" blood samples record not only the  $\beta$ -particle doses during the "irradiation" period, but bremsstrahlung during the "nonirradiating" periods. On the other hand, the chambers for the control blood samples are located in a parallel position behind the 2.5 mC plaques the whole time, and therefore their dosimeters record "leakage"  $\beta$  particles as well as bremsstrahlung. In order to determine the doses involved, it was necessary to determine the bremsstrahlung energy spectrum, since the silver-activated fluoroglass dosimeters are highly energy-dependent in this region. This was done with a 1.5 in. diameter by 1.0 in. NaI(Tl) scintillation detector and a 400-channel pulse-height analyzer. A typical spectrum is shown in Fig. 17. As expected, the peak is at the characteristic  $K$  x-ray emission from platinum. It was thus

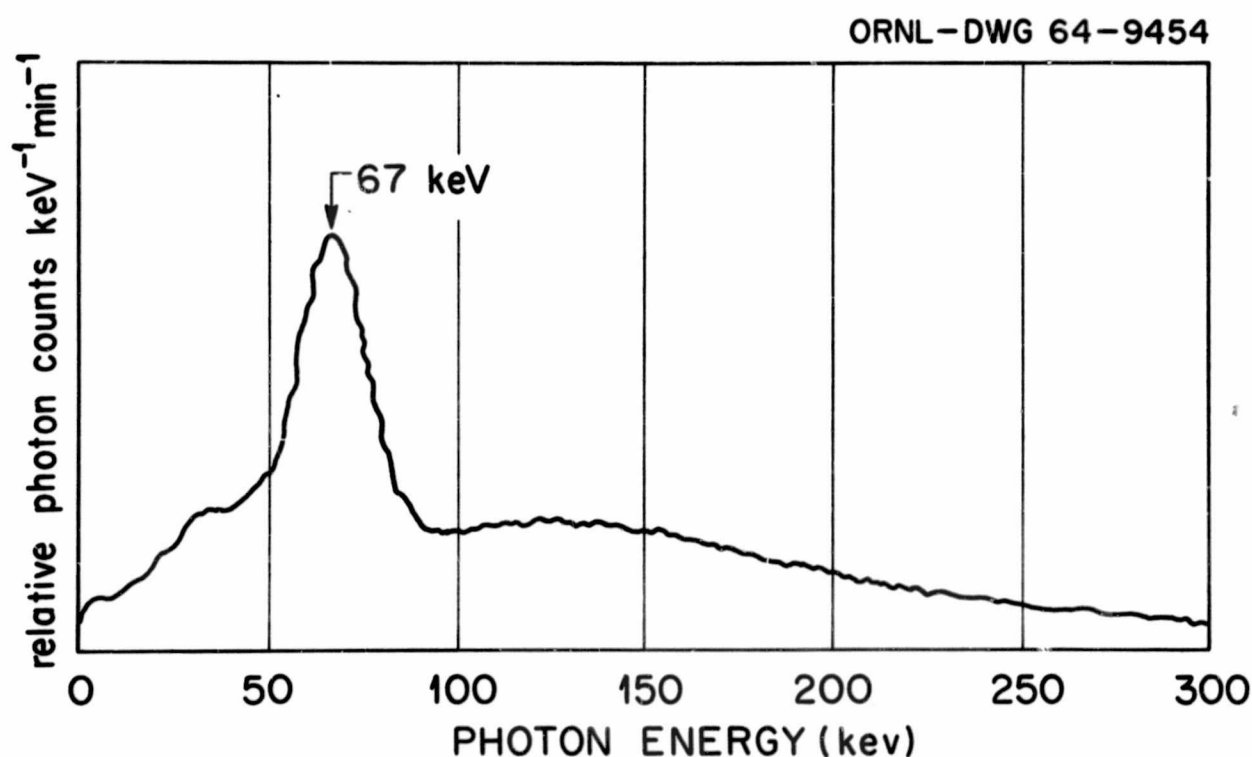


Fig. 17. Bremsstrahlung Spectrum of the S-4 Experimental Device. Peak at 67 Kev is the characteristic  $K$  x-ray emission from the platinum used for backing the  $^{32}\text{P}$  source plaques.

assumed that the dose to the fluoroglass dosimeters in the "nonirradiating" position consisted entirely of monoenergetic photons of 67 Kev. The sensitivity of the Toshiba fluoroglass used for the S-4 experiments is 4.5 times higher at this energy than it is for  $^{60}\text{Co}$  or  $^{137}\text{Cs}$   $\gamma$  rays, if the sensitivity is expressed as fluorescence yield per roentgen.

### E. Mock-up Experiments

A series of seven mock-up experiments were carried out prior to the flight. These served to test the biological and mechanical aspects of the experiment as well as the actual facilities, equipment, and supplies to be used. They also provided essential training and drill for the personnel involved. In each case the operations were carried out under as nearly the conditions anticipated for the actual GT-3 mission as possible. An exception was made, however, in the case of welding the experimental devices shut. As the unwelded devices are largely recoverable, the welding step was omitted in several of the mock-ups in the interests of economy. The mock-up experiments also varied somewhat in the times of preparation of the experimental devices, time of irradiation, and the actual source strengths at the time of irradiation, partly because the exact times, etc., could not be determined prior to the actual flight. The chromosome preparations were scored (100 cells per individual for each dose point) for all except one of the mock-up experiments. The aberration data for the fifth mock-up, which most clearly approximated the physical conditions of the actual GT-3 S-4 experiment, are given in Table 5. Iterative least-squares fits of the deletion and of the ring and dicentric data were made to the expressions

$$Y_1 = a_1 + bD, \quad (10)$$

$$Y_2 = a_2 + cD^2, \quad (11)$$

respectively, where  $Y$  is the yield of aberrations,  $a$  the spontaneous frequency,  $D$  the dose, and  $b$  and  $c$  the coefficients of deletion and ring and dicentric production. These yielded values of  $b = 5.36 \pm 0.86 \times 10^{-4}$  and  $c = 2.66 \pm 0.60 \times 10^{-6}$  per cell per rad. These values are typical

Table 5. Results of Experiment S-4 Mock-up Experiment 5

Cells Scored	Estimated Dose (rads)	$2n \neq 46$	Chromatid Deletions	Chromosome Deletions	Ring and Dicentric Chromosomes
200	2	8	2	1	0
200	47	6	2	7	1
200	97	9	4	19	9
200	138	15	5	23	22
200	189	19	2	22	32

for all of the mock-up experiments. Figure 18 shows an example of a normal mitosis without aberrations. Figures 19 and 20 show, respectively, examples of an induced deletion and an induced dicentric chromosome.

The coefficients of aberration production for the mock-up experiments are somewhat lower than had been found in previous x-ray experiments. Because there seemed no a priori reason to assume that the relative biological effectiveness (RBE) for  $^{32}\text{P}$   $\beta$  rays should be lower than that

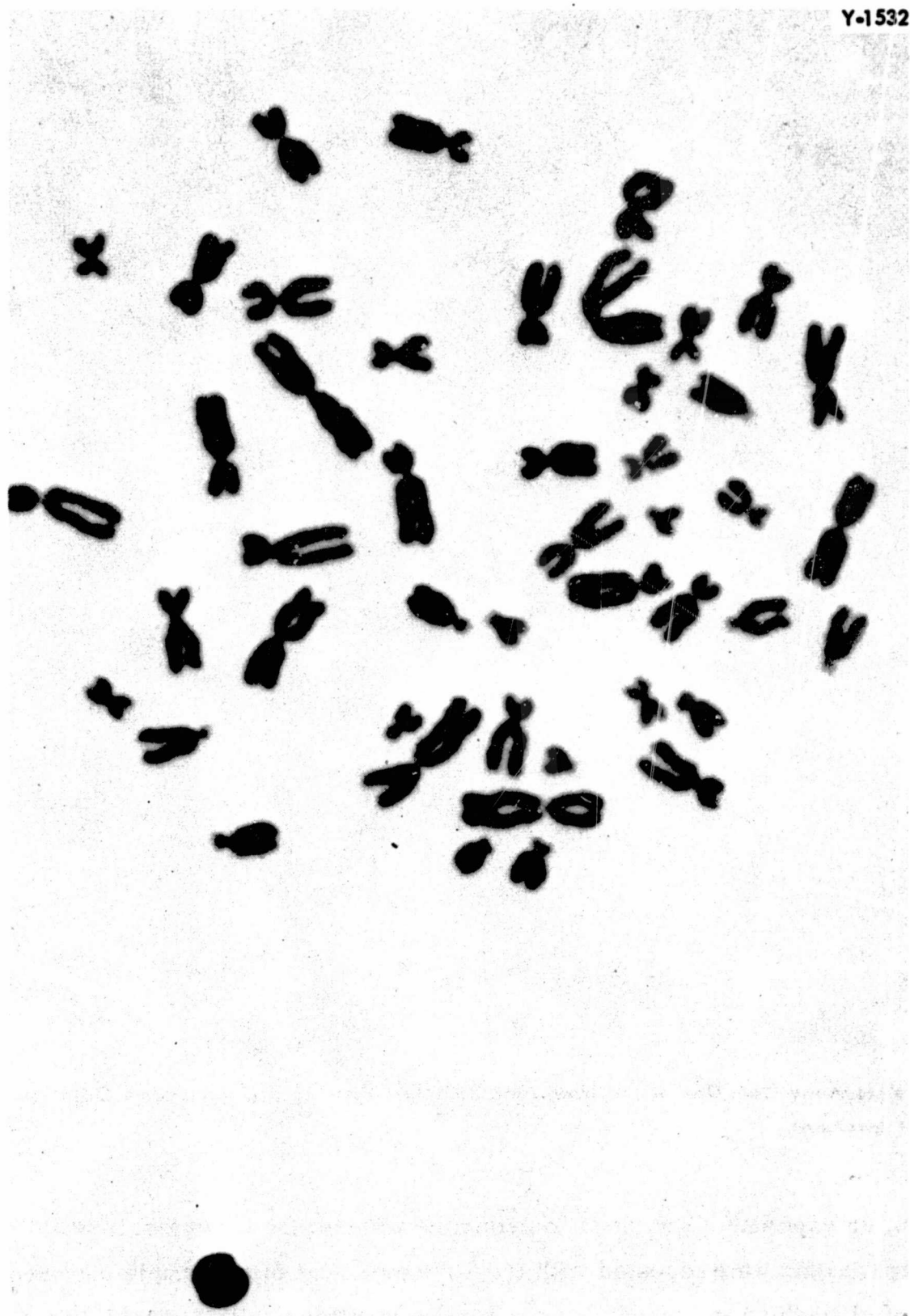


Fig. 18. Normal Metaphase Chromosomes from a Cultured Human Peripheral Leukocyte.



**Fig. 19. Metaphase from One of the Irradiated Samples Showing a Chromosome Deletion. Arrow indicates acentric fragment.**

for hard x rays, an experiment was done to determine whether the same result would be obtained if the x-ray experiments were repeated with the S-4 experiment blood-sample chambers. A 250-kv constant-potential machine was used, and the beam was filtered with 1 mm Al plus 1 mm Cu, yielding an HVL of 2 mm of Cu. Exposures were measured with a calibrated Victoreen condenser meter. The results of the experiment are shown in Table 6. Iterative least-squares fitting of the



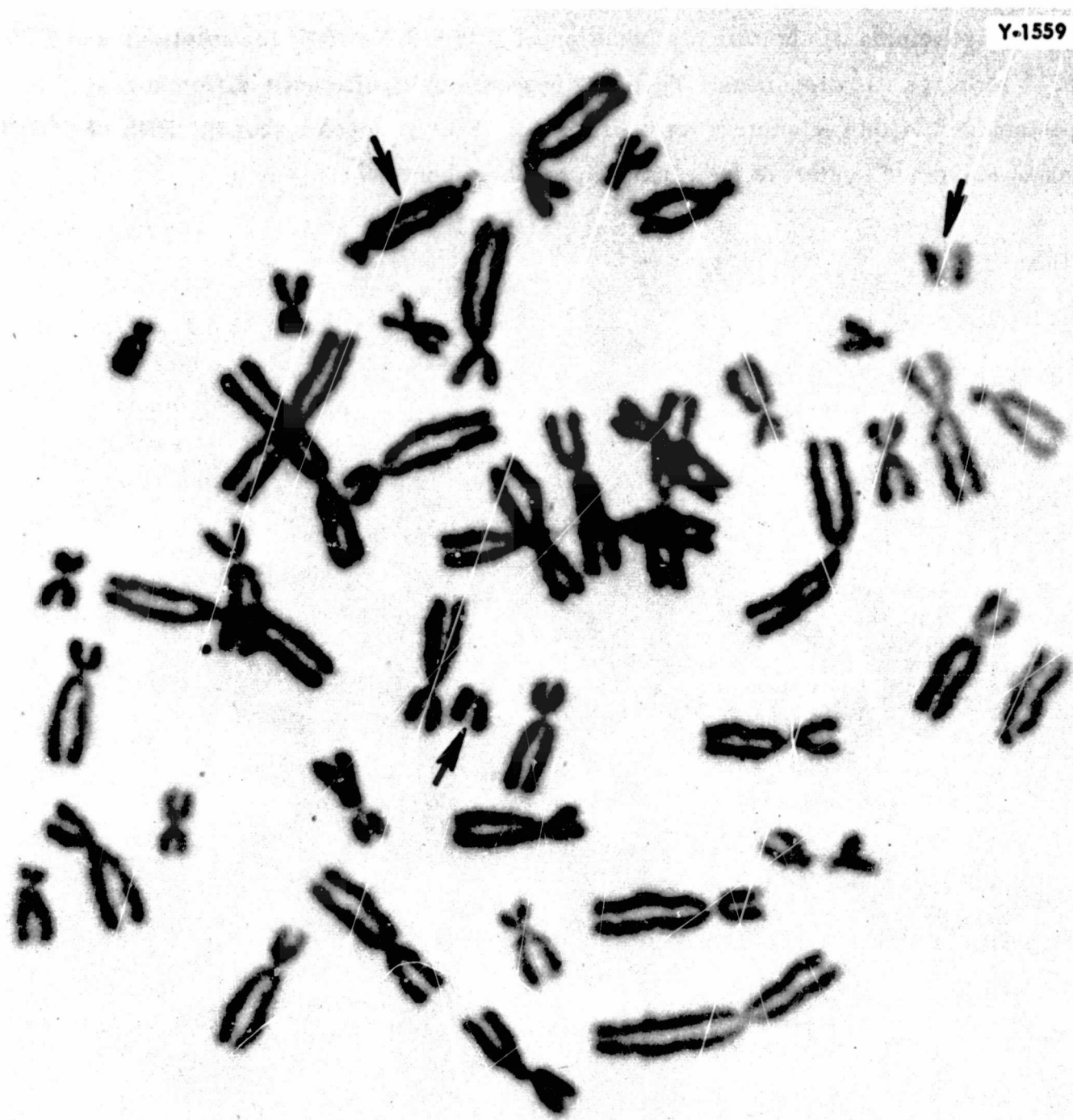


Fig. 20. Metaphase from One of the Irradiated Samples Showing a Typical Two-Break Aberration, a Dicentric Chromosome. Arrows indicate the dicentric and the acentric fragments.

Table 6. Results of Chromosome Aberration Analyses from Experiment S-4 X-Ray Test

Cells Scored	Dose (r)	$2n \neq 46$	Chromatid Deletions	Chromosome Deletions	Ring and Dicentric Chromosomes
200	0	13	1	0	0
200	50	11	5	7	6
200	100	20	5	15	25
200	150	14	2	18	22
200	200	20	2	62	35

data yielded coefficients of aberration production of  $1.36 \pm 2.2 \times 10^{-3}$  for deletions and  $1.04 \pm 0.14 \times 10^{-5}$  for rings and dicentrics. These values are not significantly different from those previously determined in this laboratory for hard x rays. Thus it appears that the RBE of  $^{32}\text{P}$   $\beta$  rays in the human leukocyte system is less than 1, probably about 0.7.

## IV. EXECUTION OF THE EXPERIMENT

### A. Preflight

About 10 days before the scheduled GT-3 launch date, the laboratory-shop trailer was located in the Hanger S area at Kennedy Space Center. A staff consisting of three biologists, two engineers, a welder, and a radiation physicist had all arrived several days before launch. The trailer equipment and facilities were checked out, and a series of test human blood cultures were made up and were fixed a week before launch. The resulting chromosome preparations were entirely satisfactory. All liaison and communications problems were satisfactorily resolved prior to launch. The launch-site staff participated in several of the mission simulations run prior to the actual flight. This served both as drill for the staff and as an opportunity for the NASA inspector who was to monitor the assembly of the actual spacecraft experimental device to become familiar with the procedures involved.

Enough flight-qualified experimental device parts were taken to the launch site to provide adequate backup for any conceivable contingency. Six complete  $^{32}\text{P}$  source-plate sets were transported to the launch site by the last staff members to arrive several days before launch was scheduled. The  $^{32}\text{P}$  source fabrication was done as late as possible because the 2-week half-life of the isotope would have necessitated use of excessive amounts of activity if they had been fabricated much in advance. An additional series of source-plate assemblies ready for  $^{32}\text{P}$  application was kept at Oak Ridge in case delays in the launching of GT-3 made it necessary to provide fresh sources.

On March 21, 1966, sterile peripheral-blood samples were obtained from the flight crew members and from the backup crew. These were put in culture in the trailer.

Several days before scheduled departure, the three recovery area biologists reported to the prime recovery vessel and to the first- and second-orbit recovery area vessels. They set up and checked their facilities, equipment, and supplies and made up and fixed blood cultures as a final test. The resulting chromosome preparations were all quite satisfactory. Prior to departure of the recovery forces, the recovery area biologists had made the necessary liaison contacts with other recovery personnel.

Approximately 9 hr before the GT-3 launch at 9:24 AM EST on March 23, sterile peripheral-blood samples were obtained from the two preselected donors (one male and one female) for the experiment. Two complete experimental devices were then assembled. Each of the sterile blood-sample-holder cavities was completely filled with blood. The chambers were sealed with the nylon screws, leaving no air bubbles within the samples. After final assembly, the experimental devices were welded shut and tested for leaks. Approximately 210 min before launch the flight experimental device was mounted in an insulated bracket located on the inside surface of the right-hand hatch. The ground experimental device was placed in a controlled-temperature cabinet, in which the temperature was periodically adjusted so that it corresponded to the temperature being read out from the spacecraft cabin.

## B. Flight

After lift-off, the spacecraft (and the flight experimental device) was subjected to two phases of longitudinal acceleration corresponding to the burning of the booster and then the sustainer engines. Acceleration rose gradually to about 5.5g at approximately +152 sec Gemini elapsed time (GET), dropped, and gradually rose again to a maximum of about 7.5g just before sustainer-engine cutoff at approximately +334 sec GET. The flight experimental device then became essentially weightless.

The irradiation of the blood samples in the flight experiment was initiated by the pilot 50 min and 18 sec after lift-off. Twenty minutes later (70 min 18 sec GET) the pilot terminated the irradiation. The corresponding activation and deactivation of the ground experimental device occurred at 52 min 0 sec and 72 min 0 sec GET respectively. The two irradiations were thus approximately 102 sec "out of phase."

After irradiation the flight experimental device remained "weightless" until retrofire and reentry, except for three brief periods of minor accelerations. These occurred during the three orbital maneuvers known as the "Texas," "lateral," and "preretro" maneuvers. The levels of these accelerations have been calculated because none produced sufficient acceleration to register on the spacecraft's accelerometers. The "Texas" maneuver started at 1 hr, 32 min, and 59 sec GET, and produced an acceleration of approximately 0.016g for 75 sec. The "lateral" maneuver started at 2 hr, 16 min, and 59 sec GET and produced an acceleration of approximately 0.011g for 26 sec. The "preretro" maneuver was begun at 4 hr, 21 min, and 23 sec GET and produced an acceleration of approximately 0.03g for 111 sec. Retrofire was begun at 4 hr, 33 min, and 23 sec, and produced four consecutive periods of acceleration of approximately 0.5g each lasting for approximately 4.5 sec, ending at 4 hr, 33 min, and 44 sec GET. During the reentry phase, acceleration built up gradually to a maximum of approximately 4.5g at 4 hr, 45 min GET. At 4 hr, 46 min, and 50 sec GET a period of vibration and accelerations on all three spacecraft axes began. It continued for 140 sec. On the two lateral spacecraft axes the vibrations reached peak amplitudes of 0.45 and 0.40g at about 4 hr, 47 min, and 10 sec GET. On the longitudinal spacecraft axis there was a peak of about 2.0g at 4 hr, 48 min, and 55 sec. These vibrations and shocks were caused by chute deployment and aerodynamic factors during the final descent of the spacecraft.

The flight experimental material, then, was subjected to the vibrations and accelerations associated with the launch phase of the flight, remained essentially weightless for 50 min prior to, 20 min during, and 3 1/2 hr following irradiation (except for three brief periods of minor acceleration), and finally experienced the accelerations and vibrations associated with retrofire, reentry, and splashdown. The ground control experimental material remained at 1g and did not experience significant vibration during these periods.

## C. Postflight

Peripheral blood samples were obtained from the Gemini-III flight crew approximately 6 1/2 hr after launch. Shortly after the spacecraft was recovered, the flight experimental device was re-



moved and opened and the blood samples were recovered. The ground experimental device was opened and the blood samples were removed at approximately the same time. All blood samples had been placed in culture by 10 hr after launch; those from the ground experiment at the launch site and those from the flight experiment on the prime recovery vessel.

The cultures of the preflight samples from the flight crew and backup crew were fixed the day after the flight, approximately 72 hr after they were made. The cultures of the experimental samples, as well as those of the flight-crew postflight samples, were all fixed at approximately 66 hr. All cultures yielded satisfactory cytological preparations. Following completion of the chromosome preparation, they, the dosimeters, and the experimental devices were returned to Oak Ridge for analysis.

## V. EXPERIMENTAL RESULTS

Careful postflight inspection of the experimental devices revealed no signs of physical damage. The housing of the S-4 experimental device as well as the blood-sample holders are partially destroyed in the process of cutting them open to recover the samples, dosimeters, etc. On inspection during the opening process, however, no signs of leakage of the blood samples or of contamination of the holders or instrumentation package with isotope were seen. The parts of the recovered flight device are shown in Fig. 21 (the corners on two of the blood-sample holders were broken after recovery, as the result of a minor accident on the recovery vessel).

### A. Instrumentation Packages

After return to Oak Ridge, the instrumentation packages from the flight and ground control experimental devices were subjected to careful analysis. The film strips were removed and developed. They were scanned with a Beckman spectrophotometer and the readings translated

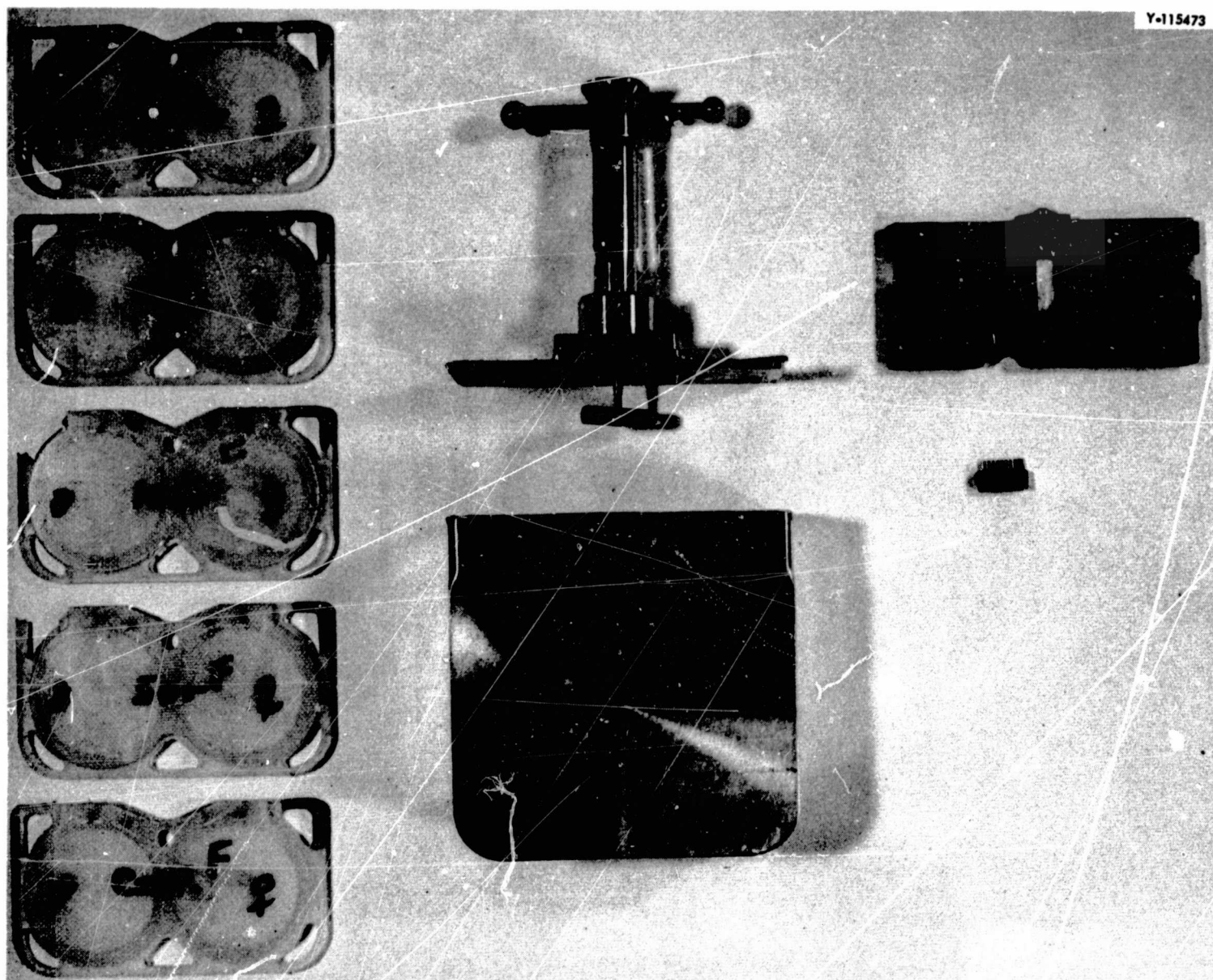


Fig. 21. Photograph of the Flight S-4 Experimental Device After Recovery and Disassembly to Recover the Blood Samples, Dosimeters, and Instrumentation Package. The corners on two of the blood-sample holders were broken on the recovery vessel, after the blood samples had been removed.

into temperature and event (irradiation) markers vs time. Both instrumentation packages were given complete postflight electrical and operational tests with the same batteries used during the actual S-4 experiment. All results compared satisfactorily with the preflight test data (see Fig. 9), and indicate that both instrumentation packages operated completely satisfactorily.

The records from the flight instrumentation package showed that when it was turned on during final assembly of the experimental device its temperature was below 28.9°C. Within the first 15 min the temperature rose above this point. For the remainder of the time until the experimental device was opened the temperature did not go above 34.4°C. The event marker appeared at the proper point and there only, indicating that only the single irradiation indicated by the GT-3 mission records took place. The duration of the irradiation did not exceed 30 min (the resolution of the instrument does not permit greater accuracy).

The records from the ground control instrumentation package showed that when it was turned on its temperature was below 29.0°C. At about the time this experimental device was welded the temperature rose to above 33.1°C. For the remainder of the time until the ground control experimental device was opened the temperature did not go above 48°C or below 17.1°C. The event marker appeared at the proper point, agreeing in time with the launch-site records.

The reason for the difference in the temperatures indicated by the two devices appears to be that the temperatures indicated for the spacecraft cabin during the flight did not actually reflect the temperature of the flight experimental device, probably because the cabin atmosphere circulating fan was not operated during the flight. The temperature of the cabinet in which the ground control experimental device was located during the flight was thus kept higher than that of the flight experimental device. However, the temperatures of the two devices were clearly within the experiment's tolerance range during the entire experiment.

## B. Dosimetry

In addition to reading the fluoroglass rods and blocks used in the GT-3 S-4 experimental devices to monitor the doses received by the blood samples, a series of postflight "reconstruction" experiments were performed with the recovered flight and ground control  $^{32}\text{P}$  sources.

Table 7 summarizes the fluoroglass rod readings for the S-4 experiment, made with the same Toshiba model B3 fluorometer used for the other dosimetry. The fluorometer was calibrated to read 0.5  $\mu\text{A}/\text{r}$  by means of fluoroglass exposed to known  $^{60}\text{Co}$   $\gamma$ -ray doses at the National Bureau of Standards. Both ends of each of the dosimeters were read, and the average was taken as the fluorescence yield. The actual dosimeters from the S-4 experiment served only to monitor the  $^{32}\text{P}$  exposure carried out during the experiment. The actual doses received by the blood samples were estimated from these fluoroglass readings by the following indirect method.

An extra set of  $^{32}\text{P}$  sources was used to measure dose rates at the "irradiation," "nonirradiating," and control positions in an experimental device. The fluoroglass rods were encased in the same type of nylon screw shanks used for the actual experiments. The rods were inserted

**Table 7. Reading of Fluoroglass Rods Used for Monitoring Radiation Doses in GT-3 Experimental Devices (Readings Are Averages of Those for the Four Dosimeters in Each Blood-Sample Chamber)**

Chamber	$^{32}\text{P}$ Activity (mC/plaque)	Flight ( $\mu\text{A}$ )	Ground Control ( $\mu\text{A}$ )
Control	0	7.6	8.8
1	$0.625 \times 0.955^a$	34.6	36.0
2	$1.25 \times 0.955$	58.4	54.6
3	$1.875 \times 0.955$	73.4	81.2
4	$2.5 \times 0.955$	88.1	99.8

<sup>a</sup>The decay factor is necessary because the sources were made to be at nominal activity 1 day before the actual GT-3 launch.

**Table 8. Fluoroglass Rod Readings for the Actual GT-3 Experiments and Those for Reconstruction Experiments Made with the GT-3 Flight and Ground Experimental Device  $^{32}\text{P}$  Plaque Sets After Recovery, and with the Duplicate Set Used for Calibration**

$^{32}\text{P}$ Activity (mC/plaque)	Glass Reading ( $\mu\text{A}$ ) for 20-Min $\beta$ -Ray Exposure after Decay Correction for $^{32}\text{P}$				
	GT-3 F Plaque Set		GT-3 G Plaque Set		Calibration Plaque Set
	Actual	Reconst.	Actual	Reconst.	
0.625	27.0	27.8	27.2	28.6	27.1
1.25	50.8	51.5	45.8	49.2	52.8
1.875	65.8	73.5	72.4	79.1	78.4
2.5	80.5	86.5	91.0	93.5	91.9

into a water-filled blood sample chamber and were either exposed for 20 min or were kept in the "nonirradiating" position for 20 hr. Similar experiments were also carried out with the recovered GT-3 flight and ground control devices. Table 8 summarizes the fluoroglass rod readings for  $\beta$  particles only for the actual flight experiments and the reconstruction experiment. For this comparison the  $\beta$ -particle dose readings of the rods in the actual ground and flight experiments were estimated from the actual overall readings given in Table 7 (which included  $\beta$  dose plus bremsstrahlung dose) by subtracting the control rod readings. The control rod readings were used to approximate the bremsstrahlung effect because the latter are in fact close to the bremsstrahlung readings obtained from the fluoroglass block dosimeters in the instrumentation packages as shown in Table 9. All the rod readings were normalized to those for the "standard"  $^{32}\text{P}$  activities originally scheduled (i.e., 0.625, 1.25, 1.875, and 2.5 mC per plaque) by applying  $^{32}\text{P}$  decay corrections. On the day of the GT-3 mission the  $^{32}\text{P}$  sources used actually had lower activities by the amount of 1 day's decay.



Table 9. Estimation of Doses for the "Standby" and Control Sample Chamber Positions in the GT-3 S-4 Experiment<sup>a</sup>

a. Data of GT-3 and Reconstruction Experiments				
Position	Experiment	Glass	Reading ( <sup>60</sup> Co γ r equiv.)	Blood Dose (rads)
Control	GT-3 flight	4 rods	7.6	>1.6
	GT-3 ground	4 rods	8.8	>1.7
	Reconst.	8 thin plates	7.2	3.4
Standby 1	Reconst.	4 rods	6.8	1.5
		4 rods	7.5	1.7
		4 rods	7.0	1.6
		4 rods	5.9	1.3
Average		6.8 ± 0.8	1.5 ± 0.2	
Instrument	GT3-F	2 blocks	2.5	~0.6
Package	GT3-G	2 blocks	1.8	~0.4

b. Depth-Dose Distribution in the Control Chamber

Depth <i>t</i> (mm)	Bremsstrahlung		β Rays, Reading and Blood Dose	Total Blood Dose (rads)
	Glass Reading (r)	Blood Dose (rads)		
0.2	6.7	1.5	9	
1.5	4.8	1.1	1.6	
2.9	3.8	0.8	0	
Average	5.1	1.1	3.5	4.6

<sup>a</sup>The actual exposures, from the time of assembly to the time of disassembly of the devices, were approximately 16 hr.

As will be seen from Table 8, the reproducibility of glass rod readings was satisfactory. The average of the differences of the fluoroglass rod readings between the reconstruction and the actual GT-3 experiments is about 3% within the same set and about 4% between the different sets. This means that the doses given to the blood samples in the GT-3 experiment are, within overall errors of about 4%, reproducible by reconstruction experiments. Therefore, the average β-particle field intensities of the three <sup>32</sup>P plaque sets were carefully compared by means of fluoroglass dosimeters as outlined earlier, and as summarized in Table 3. There were no systematic variations among the three sets. This indicated that the dose rates for either of the GT-3 <sup>32</sup>P source sets can be taken as equal to those for the "calibration" set, for which the absolute dose rates had already been estimated.

As will be seen from Table 3, there is good linearity between fluoroglass rod readings and  $^{32}\text{P}$  activities when the rods were placed within 1.5 mm of the center of the  $^{32}\text{P}$  discs. Hence, the increased nonlinearity with increasing  $^{32}\text{P}$  activity shown in Table 7 appears to be due to an increased inhomogeneity of  $^{32}\text{P}$   $\beta$ -particle distribution at the periphery of the  $^{32}\text{P}$  discs, where the rods in the blood-sample-holder plug screws were located.

Estimation of doses in the "nonirradiating" position and of the dose to the control blood samples was done from fluoroglass rod and thin-plate readings in the postflight reconstruction experiments. It was assumed that the rod readings at the standby positions were entirely due to the bremsstrahlung from the platinum source backing. The increased fluorescence yield for photons of 67 Kev had already been determined experimentally to be 4.5 times that for  $^{60}\text{Co}$  and  $^{137}\text{Cs}$   $\gamma$  rays. The rough estimate of tissue dose (rads) for the blood samples in the "nonirradiating" position was thus made simply by dividing the readings for the fluoroglass (in r units of  $^{60}\text{Co}$   $\gamma$ -ray exposure equivalent) by 4.5. Because the reconstruction experiment exposure time was 20 hr, the readings were also multiplied by the factor of  $\frac{4}{5}$  after  $^{32}\text{P}$  decay corrections so as to match the approximate 16-hr "nonirradiating" position period in the actual GT-3 experiments. The results are summarized in Table 9a. The estimated blood dose during the time spent at the "nonirradiating" position is 1.5 rads.

The dose for the blood samples at the control position is more difficult to estimate because it is due to a mixed field of  $\beta$  particles and bremsstrahlung. The depth-dose method with 0.14-mm-thick fluoroglass plates, already described in Sect. IIID above, is applicable for separation of  $\beta$ -ray dose from bremsstrahlung dose, since the latter decreases only slowly with depth in the sample. The bremsstrahlung dose component was estimated from the overall depth-dose readings by applying the following depth-dose formula:

$$Y \propto \log [1 + (t/a)^2], \quad (12)$$

where  $Y$  is the bremsstrahlung dose at depth  $t$  (mm) in the blood-sample phantom and  $a$  the radius of the  $^{32}\text{P}$  source disc. The overall glass readings at  $t = 3$  mm were assumed to be entirely due to bremsstrahlung. Conversion of the fluoroglass readings for the bremsstrahlung by dividing by 4.5 (as before) gave rough estimates of the tissue dose due to bremsstrahlung. These results are given in Table 9b. The final value indicates a control dose-rate of about 3.5 rads during the 16-hr period. The sum of glass readings for both bremsstrahlung and  $\beta$  particles (in r units of  $^{60}\text{Co}$   $\gamma$ -ray exposure equivalent),  $4.8 + 2.4$  gave the 7.2 (r) value as the reconstructed overall rod reading in the control position, which is in fairly close agreement with the actual values of 7.6 and 8.8 (r) for the GT-3 flight and ground control experiments as shown in Table 9a.

Table 10 summarizes the estimates of the doses to the blood samples in the GT-3 S-4 experiment obtained by all methods. It will be seen that they are in reasonably good agreement. A summary of our best estimates of the doses actually received is given in the last column of Table 10. These estimates were used for the calculation of coefficients of aberration production for the experiment.

Table 10. Summary of "Best" Overall Dose Estimates for Samples Exposed in the S-4 Experiments Carried Out During the GT-3 Mission

<sup>32</sup> P Nominal Activity	$\beta$ -Ray Dose (rads)				Bremsstrahlung Dose (rads)	Overall Blood Dose (rads)
	Theory	Glass	Fricke	Average		
Control		2.4		2.4	1.1	4
0.598	45	47.4	48.8	47	1.5	49
1.20	90.6	92.0	94.6	92	1.5	94
1.79	135.5	139	142	139	1.5	141
2.39	180.5	177	190	183	1.5	185

### C. Biological

The results of the chromosomal aberration analyses are shown in Table 11. The frequencies of chromatid aberrations and of cells with chromosome numbers other than  $2n = 46$  (excluding those with aberrations) are not different from those seen in other experiments; the average values in our laboratory are 1.3% chromatid-type aberrations and 4.9% cells with  $2n \neq 46$ , but values of  $2n \neq 46$  are quite variable, and frequencies as high as 15% are sometimes seen. The two chromosome deletions seen in the samples from crew member "B" are not significant; in cells from normal control persons examined in our laboratory the frequency of chromosome deletions is 0.5%. The two dicentric chromosomes seen in the samples from the same crew member appear to be identical. No acentric fragments accompanied either dicentric. It seems likely that they are members of an established clone, but in any case it is clear that they are "old" aberrations, having nothing to do with the space flight.

Two hundred cells were scored from each sample from each donor. There were no significant differences between samples from the two donors, and they have consequently been pooled in Table 11.

The frequencies of chromosome-type aberrations in the control samples are quite consistent with the low dose they received (from  $\beta$ -particle leakage and bremsstrahlung within the experimental devices) during the course of the experiment. Although not deliberately irradiated like the other experimental samples, they are not in reality "unirradiated controls" either. The frequencies of two-break ring and dicentric aberrations appear very similar; certainly there is no consistent difference between their frequencies in the series of irradiated samples. The frequencies of the single-break chromosome deletions, on the other hand, do show a consistent difference when the flight and ground samples are compared: the chromosome-deletion yields for the ground portion of the experiment are lower in all four dose groups.

The data in Table 11 were fitted to the expressions (10) and (11) by iterative least-squares regression analysis in order to determine the values of  $b$  and  $c$  for the ground and flight portions



Table 11. Results of Experiment S-4 Chromosome Aberration Analyses

Subject	Sample	Cells Scored	Est. Dose (rads)	$2n \neq 46$	Chromatid Deletions	Chromosome Deletions	Ring and Dicentric Chromosomes
<b>Crew</b>							
A	Preflight	100		8	3	0	0
	Postflight	200		8	2	0	0
B	Preflight	100		4	0	1	1 <sup>a</sup>
	Postflight	200		7	0	1	1 <sup>a</sup>
<b>Experiment</b>							
	Gr	400	4	31	3	3	1
	F1	400	4	33	1	3	0
	Gr	400	49	20	1	6	5
	F1	400	49	26	3	14	1
	Gr	400	94	22	5	13	13
	F1	400	94	24	6	28	16
	Gr	400	141	20	6	32	43
	F1	400	141	44	6	48	34
	Gr	400	185	38	6	45	36
	F1	400	185	58	2	88	48

<sup>a</sup>These two dicentric chromosomes appear identical; both lacked acentric fragments.

of the experiment. The results are shown in Table 12, together with those from mock-up experiment 5. It will be seen that the yields for ring and dicentric chromosomes in the flight and ground experiments and for chromosome deletions in the ground experiment agree well with the results of the previous "control" experiment. The ring and dicentric yields for the flight and ground experiments do not differ significantly from each other. The yield of chromosome deletions in the flight portion of the experiment, however, is almost twice that seen in either the ground experiment or the previous control experiment. The difference is significant ( $P \approx 0.0005$ ) and, as already pointed out, completely consistent.

The data for chromosome deletions for both parts of the experiment show a noticeable departure from the linear dependence on dose assumed in calculating the coefficients of deletion production shown in Table 12. This has been true of the deletion data from all of our preflight mock-up experiments as well. We therefore also fitted the S-4 deletion data to a quadratic model of the form

$$Y = b_1 D + b_2 D^2, \quad (13)$$

where  $b_1$  and  $b_2$  are the new coefficients of deletion production. These values are shown in Table 13. Because the new coefficients are smaller, and their standard errors larger, it is not possible to demonstrate a significant difference between the ground and flight values of either coefficient. It is apparent, however, that while both coefficients are larger for the flight portion of the experiment,  $b_1$  has increased at least as much as  $b_2$  ( $2.3\times$  vs  $1.6\times$ ).

Table 12. Coefficients of Aberration Production for S-4 Experiment

	Deletions ( $\times 10^4$ ) per Cell per Rad	Rings and Dicentrics ( $\times 10^6$ ) per Cell per Rad <sup>2</sup>
Ground Control	4.79 $\pm$ 0.72	3.23 $\pm$ 0.59
Flight	9.11 $\pm$ 1.02	3.48 $\pm$ 0.53
Run 5	5.36 $\pm$ 0.86	2.66 $\pm$ 0.60

Table 13. Fits of S-4 Deletion Data to the Model

$$Y = b_1 D + b_2 D^2$$

	$b_1$ ( $\times 10^4$ )	$b_2$ ( $\times 10^6$ )
Ground Control	1.8 $\pm$ 1.4	2.3 $\pm$ 1.0
Flight	4.2 $\pm$ 1.7	3.7 $\pm$ 1.2

Included in the chromosome-deletion class is one group, the interstitial deletions, which are generally believed to require two separate breakage events. These are infrequent in human material, however, and cannot have contributed much to the second-order deletion component. In the S-4 experiment only 11 were observed in the ground portion, evenly distributed through the total of 2000 cells scored in all dosage groups. A total of 17 were observed in the flight portion of the experiment, again evenly distributed in the various dose groups.

#### D. Discussion

It is clear that the S-4 experiment failed to demonstrate any unprecedented effect of the small amount of ambient radiation encountered by the spacecraft during flight. No aberrations attributable to the flight were found in the blood samples from the crew. Further, the few aberrations seen in the flight control samples can readily be accounted for by the small radiation dose they received from the <sup>32</sup>P sources during the flight.

The greater yield of aberrations seen in the flight experiment than in the ground experiment is difficult to explain. It is always possible, of course, that the difference is simply a sampling artifact, even though the probability is very low. If the difference is real, however, it seems likely that some space-flight parameter was involved and that, in fact, some synergism does exist

(whether synergism is the strictly correct term to apply is really academic; the term will in any case be understood in the present context).

The extensive dosimetric work done for the S-4 experiment rules out the possibility that the doses received by the blood samples were actually significantly different. And even if the doses were different, the biological results would not be explained, since one would expect the yields of *all* classes of chromosome aberrations to be greater. In fact, the increase should be larger for the two-break aberrations, because of their more nearly second-order dose-effect kinetics. The same argument applies to the possibility that the doses to the *individual cells* in the flight experiment might have been different because of some difference in the spatial distribution of the cells within the sample volume. If, for example, the cells in the blood samples of the flight experiment had tended for some reason to become located next to the "windows" of the blood-sample chambers, the average dose to the cells would have been larger than if they had been distributed evenly through the "depth" of the chambers. Again, however, the yields for *all* aberrations should have been increased.

Temperature and oxygen tension are both known to influence induced chromosomal aberration yields, but neither factor could be expected to produce the differential effect seen in the S-4 experiment. Furthermore, neither factor can actually have been very different in the two parts of the experiment. The ambient temperatures for the two experimental devices, although not identical, were similar; only during the welding was there a significant departure from "room temperature" for either device. All of the blood samples were somewhat anoxic at the time of irradiation, owing to their having been sealed up in the blood-sample chambers without any gaseous oxygen supply for about 9 hr. Since all of the chambers were sealed up at one time, however, there cannot have been any significant, consistent difference between the degree of anoxia of the samples in the two parts of the experiment.

Another approach to explaining the results of the S-4 experiment is to look for deviations from what might be expected in the results of the ground portion of the experiment. This has not been particularly rewarding, however. One such difference is the rather low coefficients of aberration production observed. Another lies in the kinetics of aberration production. As mentioned already, "control" experiments were carried out before the flight. A total of seven mock-up experiments were carried out, using the same experimental devices used for the actual S-4 experiments. Variations in timing, source strength, etc., were necessary because these factors could not be known exactly for the S-4 experiment until the GT-3 flight was actually accomplished. Thus only one of the "control" experiments is really exactly comparable to the S-4 experiment. As shown in Table 12, however, the results agree with those of the ground portion of the S-4 experiment. Furthermore, *all* of the preflight experiments agreed in that the aberration yields were low, that there was a noticeable second-order component in the chromosome deletion dose-effect curve, and that there was some evidence of saturation in the two-break aberration yields (see Table 11). All three are thus clearly characteristics of the experimental setup, and cannot be considered anomalous results in the S-4 experiment. Although a detailed discussion is out of place here, it is interesting that



in the experiment in which the same blood-sample chambers were used, but in which x radiation was substituted for the  $^{32}\text{P}$   $\beta$  radiation, we obtained results in good agreement with our extensive experiments on the induction of chromosomal aberrations in x-irradiated human leukocytes. The low relative biological effectiveness (the average is about 0.7) and the kinetics are thus apparently not characteristics of the blood-sample holders or of anoxia of the blood samples.

It seems to us that there is little choice but to accept the results of the S-4 experiment as a demonstration of a synergism between radiation and some other parameter associated with orbital space flight. Whether the effect is due to "weightlessness" or vibration or some other parameter, or to a combination of factors, cannot be decided at this point. The launch and reentry acceleration and vibration profiles and the "weightlessness" during orbital flight certainly seem the most likely suspects. Many of the Russian experimenters believe that the effects they have observed following space flights are in fact vibration effects. It should be pointed out, however, that in most cases the effect of vibration in the Russian experiments must have been to produce the effect measured, and not to enhance the effectiveness of a significant radiation exposure. No such effect was observed in the S-4 experiment. In any case, it is difficult to see how very much vibrational energy can have been transmitted to the cells in the S-4 experimental device, as coupling within the device is poor, and the device was surrounded by a layer of insulating plastic foam within its mounting bracket on the spacecraft hatch.

Additional experiments will be necessary in order to help decide which factors were responsible for the effect observed in the S-4 experiment. Unfortunately, vibration and acceleration experiments will never decide the issue conclusively, because it is impossible to duplicate the GT-3 profiles exactly, both because they are not known with sufficient accuracy and because they could not in any case be reproduced in all three axes simultaneously. Nevertheless, a ground-based experiment using the best possible approximation of the vibration and acceleration profile for the S-4 flight experiment is being carried out. The best test of the possibility that the effect is due to weightlessness would be to fly duplicate experiments on some future orbital mission, keeping one of them at  $1g$  throughout the orbital phase of the flight, perhaps by centrifugation. Unfortunately, such an experiment does not seem to be technically feasible at present.

In the absence of evidence as to just which space-flight parameter or parameters were responsible for the effect, it seems futile to speculate on the exact mechanism by which they might operate. It may be pointed out, however, that whatever factors were responsible it seems extremely unlikely to us that they operated by increasing the effectiveness of the  $\beta$  particles in breaking chromosomes. It appears much more reasonable to assume that they operated by "saving" some of the many breaks or potential breaks which are normally "repaired" before metaphase, thus allowing a higher proportion of the primary lesions to reach metaphase as overt breaks and be scored as deletions. Such an interpretation is far from satisfactory, however, because it might then be expected that a marked effect would be seen on two-break aberrations, which was not in fact observed. Thus, although it seems in an intuitive sense that either vibration or "weightlessness" might, by affecting the distribution and movement of chromosomes and of broken ends

within the nucleus, influence the number of primary breakage events actually realized as scorable deletions, this is not only not really an explanation, but suffers the additional defect of creating more problems than it solves.